

A REVIEW OF THE PHENOMENON OF STRESS RUPTURE IN HDPE GEOGRIDS

GEO REPORT No. 19

G.D. Small & J.H. Greenwood

**GEOTECHNICAL ENGINEERING OFFICE
CIVIL ENGINEERING DEPARTMENT
HONG KONG**

A REVIEW OF THE PHENOMENON OF STRESS RUPTURE IN HDPE GEOGRIDS

GEO REPORT No. 19

G.D. Small & J.H. Greenwood

**This report was originally produced in September 1992
under Consultancy Agreement CE 19/89**

© Hong Kong Government

First published, June 1993
First Reprint, April 1995

Prepared by:

Geotechnical Engineering Office,
Civil Engineering Department,
Civil Engineering Building,
101 Princess Margaret Road,
Homantin, Kowloon,
Hong Kong.

This publication is available from:

Government Publications Centre,
Ground Floor, Low Block,
Queensway Government Offices,
66 Queensway,
Hong Kong.

Overseas orders should be placed with:

Publications (Sales) Office,
Information Services Department,
28th Floor, Siu On Centre,
188 Lockhart Road, Wan Chai,
Hong Kong.

Price in Hong Kong: HK\$56

Price overseas: US\$9.5 (including surface postage)

An additional bank charge of **HK\$50** or **US\$6.50** is required per cheque made in currencies other than Hong Kong dollars.

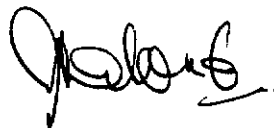
Cheques, bank drafts or money orders
must be made payable to **HONG KONG GOVERNMENT**

PREFACE

In keeping with our policy of releasing information of general technical interest, we make available some of our internal reports in a series of publications termed the GEO Report series. The reports in this series, of which this is one, are selected from a wide range of reports produced by the staff of the Office and our consultants.

Copies of GEO Reports have previously been made available free of charge in limited numbers. The demand for the reports in this series has increased greatly, necessitating new arrangements for supply. In future a charge will be made to cover the cost of printing.

The Geotechnical Engineering Office also publishes guidance documents and presents the results of research work of general interest in GEO Publications. These publications and the GEO Reports are disseminated through the Government's Information Services Department. Information on how to purchase them is given on the last page of this report.

A handwritten signature in black ink, appearing to read 'A. W. Malone', with a stylized flourish at the end.

A. W. Malone
Principal Government Geotechnical Engineer
April 1995

FOREWORD

This report presents the results of an in-depth literature review of the phenomenon of stress rupture in HDPE geogrids. Existing data for Tensar SR2, SR55, SR80 and SR110 geogrids are compiled and reviewed. The contributory factors to the material partial safety factor are also reviewed.

The study was carried out by Mr G.D. Small and Dr J.H. Greenwood of ERA Technology Limited as consultants to the Geotechnical Engineering Office (GEO) (formerly the Geotechnical Control Office) of the Civil Engineering Department. It forms part of the GEO research programme on reinforced fill structures.

The draft report was reviewed by Dr P.L.R. Pang and the Endorsement Checking Panel for Proprietary Products for Reinforced Fill Structures of the GEO. Mr J.M. Shen contributed to the finalization of the report. Whilst the findings in the report are generally accepted by the reviewers, details of the methods for the assessment of the existing stress rupture data for Tensar products are specific methods used by ERA for the present study and should not be regarded as standard methods accepted by the GEO.



(M.C. Tang)
Acting Government Geotechnical Engineer/Development
June 1993

CONTENTS

| | Page No. |
|---|-------------|
| Title Page | 1 |
| PREFACE | 3 |
| FOREWORD | 4 |
| CONTENTS | 5 |
| SUMMARY | 7 |
| 1. INTRODUCTION | 8 |
| 2. AREAS OF INVESTIGATION | 8 |
| 3. THE STRUCTURE OF POLYETHYLENE | 9 |
| 4. 'BRITTLE FAILURE' IN UNORIENTED POLYTHYLENE | 10 |
| 5. POLYTHYLENE PIPES | 10 |
| 6. FAILURE OF UNORIENTED POLYETHYLENE (MOLECULAR ASPECTS) | 11 |
| 6.1 Ductile and 'Brittle' Failure Mechanisms | 11 |
| 6.2 Environmental Effects | 12 |
| 6.3 The Effect of Molecular Structure | 13 |
| 7. THE STRUCTURE OF DRAWN AND ULTRA HIGH MODULUS POLYTHYLENE | 14 |
| 8. OBSERVED STRESS RUPTURE IN POLYETHYLENE GEOGRIDS | 15 |
| 8.1 Available Data | 15 |
| 8.2 Extrapolation of Time to 10% Strain and Time to Rupture | 16 |
| 8.3 Curve Fitting | 17 |
| 8.4 Comments on the Calculations | 21 |
| 8.5 Evidence of 'Brittle' Failure | 21 |
| 8.6 Fractures in the 'Node' Areas | 22 |
| 8.7 Is There a 'Knee' in the Rupture of Geogrids? | 22 |
| 9. RECOMMENDATIONS FOR DESIGN PROCEDURES | 25 |

| | Page No. |
|---|-------------|
| 9.1 Design Loads | 25 |
| 9.2 Safety Factors | 25 |
| 9.2.1 General | 25 |
| 9.2.2 Scatter of Extrapolation, Uncertainty in the Method of Extrapolation | 26 |
| 9.2.3 Synergy between Load and Danger Effects | 26 |
| 9.2.4 Environmental Stress Cracking (Synergy between Load and Environmental Effects) | 26 |
| 9.2.5 Possible Change in Rupture Mechanism | 26 |
| 9.2.6 Effects of Temperature Greater than 35°C | 27 |
| 9.2.7 Dynamic Loading | 27 |
| 9.2.8 Probability of the Material Strength being less than its Characteristic Value | 27 |
| 9.2.9 Dimensional Effects on Strength | 27 |
| 10. CONCLUSIONS | 28 |
| 11. RECOMMENDATIONS FOR FURTHER WORK | 29 |
| 12. REFERENCES | 29 |
| LIST OF TABLES | 34 |
| LIST OF FIGURES | 38 |

SUMMARY

ERA Technology Limited have been commissioned by the Geotechnical Control Office, Hong Kong Government Civil Engineering Services Department, to carry out an in depth literature review of the phenomenon of stress rupture in HDPE geogrids.

This report which contains the results of this review covers the failure mechanisms of unoriented polyethylene and a review of relevant research work undertaken by the gas supply industry.

The failure process on a molecular level is then introduced and discussed in the context of drawn and oriented polyethylene materials. It is concluded that where there is scope for further change in the molecular structure in a polyethylene product there must also be the possibility of a change in failure mechanism. Tensar grids are intermediate in structure between unoriented material and highly drawn films and fibres.

Existing data for Tensars SR55, SR80 and SR110 are compiled and normalised with respect to the ultimate (short-term) tensile strength of the product. Tensar SR2 is treated separately. A stress-rupture curve is calculated by time-temperature shifting to 35°C. Curves are fitted using a double logarithmic relation to give extrapolated design loads for these products. The contributory factors to the material partial safety factor f_m are reviewed.

The possibility of a change in failure mechanism, leading to a reduction in extrapolated lifetime, is then discussed. It is concluded that on existing evidence this is unlikely for Tensar geogrids.

Stress-rupture testing is required to substantiate the conclusions.

1. INTRODUCTION

Polyethylene grids for soil reinforcement are manufactured by drawing a pierced roll of high density polyethylene into highly oriented ribs between 'nodes' of lightly drawn material. The design criterion for the use of such materials in reinforced soils may be based on long term strength or long term strain. When these materials are subjected to a simple tensile test, the elongation at break is greater than 20%. Such movement would be totally unacceptable in a reinforced soil structure, so that strain rather than strength will be the critical design parameter.

There remains, on the other hand, uncertainty concerning the possibility of fracture in these grids at much lower strains at very long durations. One reason for this is the behaviour of high density polyethylene gas pipes in which there is a transition from high-strain ductile to low-strain brittle behaviour at long durations. The consequences of sudden failure occurring in a highly populated area such as Hong Kong could be so catastrophic that it is essential that any such possibility must be excluded.

Following an exchange of correspondence between ERA and the Geotechnical Control Office (GCO) of the Hong Kong Government Civil Engineering Services Department, ERA Technology Limited was commissioned to carry out an in-depth literature review of the phenomenon of stress-rupture in HDPE grids.

This report covers the findings of the literature review undertaken and presents ERA's opinion on the ability to avoid stress-rupture of polyethylene geogrids by appropriate design.

2. AREAS OF INVESTIGATION

There is very little information available in the published literature on stress-rupture or environmental stress cracking of polyethylene geogrids. Throughout this report, extensive reference has been made to Netlon Ltd's 'Tensar' range of geogrid products. Four products from this range, SR110, SR80, SR55 and SR2 grids are fabricated from high density polyethylene (HDPE).

ERA is aware of only one other source of geogrid products manufactured from HDPE. This is the Tenax range manufactured by RDB Plastotecnica SPa, Italy. The grid is marketed as a reinforcement for weak soil, a slope stabiliser, and a concrete/sub-asphalt reinforcement.

Tenax TTI, which is longitudinally drawn, is broadly similar to Tensar grids in appearance but on examination the two can be easily distinguished : Tenax TTI has significantly larger node areas and in comparison to Tensar products its shape and dimensions are less regular; furthermore, it is more flexible (especially in the nodal regions) than the Tensar counterparts. Tenax TTI has a breaking strength of 59 kN/m at 17% strain which makes it a lower strength, higher flexibility product than Tensar.

Results received by ERA show creep data at approximately 20, 40 and 60% of breaking load for Tenax grids TT201, 301, 401 and 20 and 40% for TT601 and 701. The results, to 10^4 hours, are interesting since those at 60% of breaking load indicate an approach to secondary creep while at the lower loads the rate of creep decreases rapidly. No ruptures

were observed in spite of strains of up to 40% when the test was terminated. Tenax products have therefore not been considered further in this report.

Manufacturer's data on the creep performance of Tensar geogrids and estimates of lifetime are based on a 10% strain limit and only a limited number of tests have been allowed to continue to failure. Consequently it has been necessary to survey all relevant information on fracture of polyethylene. Much of the research work on stress cracking of polyethylene has been carried out by the gas supply industry where unoriented polyethylene pipe finds extensive use in the distribution network.

The following report introduces polyethylene in terms of its characteristics and molecular structure and then covers the ductile and 'brittle' failure in unoriented material. The report then covers the 'brittle' failure in polyethylene pipes and goes on to discuss the failure process in molecular terms. The argument for and against 'brittle' failure and early rupture of oriented geogrids is then presented.

3. THE STRUCTURE OF POLYETHYLENE

All polymers consist of long molecular chains of covalently bonded atoms, one of the simplest being polyethylene, which is a semicrystalline polymer. The polymer molecules consist of long chains of ethyl groups (CH_2) and may be produced in linear or branched form. Branches may be of varying length and this affects the ability of the molecules to pack closely together.

In linear polyethylene where there are no branches the molecules may be packed closely together thereby increasing the density. Such materials are referred to as HDPE (high density polyethylene).

Many grades of polyethylene are commercially available both in branched or linear form. Grades often differ in :

- (a) average molecular weight and weight distribution,
- (b) melt index,
- (c) crystallinity,
- (d) co-monomer type and content, and
- (e) additives (eg uv stabilisers) (Ref.1)

The microstructure of polyethylene can be considered as a distribution of crystallites of varying size situated within a matrix of amorphous material.

The crystallites themselves are made up of molecules folded in a regular manner (Ref.2). The crystallites are lamellar in form and the lamellae are of microscopic dimensions. The spherulitic structure observed is formed where dominant lamellae grow from a central nucleus in all directions by twisting along fibrils (Ref.3). The intermediate spaces are filled by subsidiary lamellae, tie molecules, molecular loops and HDPE in the amorphous form.

There are various models proposed for how crystallites are held together but there is

good evidence to suggest that the molecules join one crystallite to another passing throughout the amorphous matrix and that these tie molecules are essential to hold the structure together (Ref.4).

The Tensar polyethylene grids are understood to consist of pipe grade polyethylene copolymer of 60-65% crystallinity.

4. 'BRITTLE FAILURE' IN UNORIENTED POLYETHYLENE

The mechanical properties of unoriented polyethylene, like all other polymeric materials, depend on the test conditions; for example temperature and strain rate. Furthermore, when measured under identical test conditions properties can vary as a function of molecular weight, degree of crystallinity, molecular orientation and the presence of copolymers. Under conditions of constant stress, polyethylene continues to deform with the passage of time until failure occurs. At high levels of stress where time to failure is relatively short there is a large deformation prior to failure, the strain at failure often exceeds 300%. This type of failure is termed 'ductile'. For low levels of stress where failure occurs after much longer periods of time it is not preceded by any significant deformation; strain at failure under these circumstances has been reported to be in the range 5 to 35% (Figure 1) (Refs.5, 6, 7). Although on a macroscopic scale there is little evidence of deformation prior to failure the failure surface appears ductile when viewed at high magnification (Refs.8, 9).

This lower strain failure process has been termed 'brittle' but in engineering terms a strain at failure of 10% would not normally be termed brittle. (True brittle failures of glasses and ceramics for example typically occur at strains below 2% and similar failures can be seen in polymers at very low temperatures.)

The process of 'brittle failure' which includes slow crack growth should also not be confused with environmental stress cracking of polyethylene where brittle failure occurs at reduced stress levels when the material is under load and within a stress cracking environment (Ref.10).

The 'brittle' stress-rupture effect can occur in otherwise inert environments.

Parallels have been drawn between slow crack growth and environmental stress cracking and one is often used to evaluate the other : this is covered in a later section.

No conclusions concerning the strain at failure of drawn polyethylene should be drawn from the behaviour of unoriented polyethylene.

5. POLYETHYLENE PIPES

Much of the research work carried out over the last 20 years on the brittle fracture of polyethylene has been on behalf of the gas supply industry where medium density polyethylene (MDPE) has become the most widely used pipe material for the gas distribution network. The advantages of this material are its high ductility and the ability to join pipes and fittings by thermal fusion (Ref.11).

The acceptance criterion for these pipes is that they should have a useful life of 50 years without leakage or burst (Ref.12). Research has therefore been based on pressure testing over long periods of time in usage environments at ambient and elevated temperature in order to be able to predict a safe usage stress for 50 year operation.

All work in this area has clearly shown the existence of a 'knee' in the stress-rupture curve for all grades of material (Figure 2). At the knee there is an abrupt change of slope : in the 'shallow' portion of the curve, region A, the failures are all ductile while in the 'steep' part of the curve, region B, the failures are all brittle. The knee itself is surrounded by a transition zone but represents a fundamental change in failure mechanism (Refs. 8, 12, 13). Greig (Ref. 12) has shown the potential dangers of using test data obtained at ambient temperature for predictive purposes. Clearly if the test is of insufficient duration a knee would not be encountered and an extrapolation of the stress-rupture curve to 50 years could lead to a gross overestimate of the safe operating stress level (Figure 3). Testing of the same pipes at elevated temperature and/or in a hostile environment lowers the stress-rupture curve and shifts the knee to shorter times allowing curves of various temperatures to be superposed to obtain predictions for service at lower temperatures and longer times (Figure 4). Research has shown that the position of the knee and the slope of the steep section of the stress-rupture curve is highly dependent on the environment (Ref. 13) and that wetting agents for water can shift the knee to shorter times. Where tested in media other than water the stress-rupture curves are parallel but may be situated either side of the water curve. Ifwarson (Ref. 14) has shown that air is a more aggressive environment than water and that the slope of the steep section of the curve is five times greater than when tested in water.

Stress-rupture testing of pipes has shown clearly that for a wide range of materials and environments the slope of the shallow part of the curve is always of the same order of magnitude (Refs. 13-17). A much wider variation of results however is obtained for the brittle failure region. Gaube et al (Ref. 18) found that improvements in the base polymer, for example increasing the melt flow index, 'push' the knee out to longer times while adequate quality control is essential in avoiding early brittle failure (Refs. 12, 19, 20, 21). Removal of large particles prior to extrusion by sieving reduces the incidence of critical flaws and thereby enhances the lifetime of the product; these large particles may be of base polymer or agglomerates of stabiliser. Sieving is always carried out during extension of sheet for Tensar grid manufacture.

6. FAILURE OF UNORIENTED POLYETHYLENE (MOLECULAR ASPECTS)

6.1 Ductile and 'Brittle' Failure Mechanisms

In this section the process of failure of unoriented polyethylene, on a microscopic and molecular scale, is discussed and ways of improving the resistance to long term brittle failure are reviewed.

As discussed in an earlier section, the exact molecular arrangement within polyethylene crystallites has not yet been deduced conclusively and is still an area of much research activity. In general there is a consensus of opinion that the material consists of lamellar crystallites within an amorphous matrix and that these crystallites are linked by tie molecules and tie molecule entanglements. Tie molecules begin and end in adjacent lamellae (Figure 5).

The following descriptions of ductile and brittle failure are as proposed by Lustiger and Rosenberg (Ref. 8).

When a high constant tensile stress is applied to the material, normal to the faces of the lamellae the tie molecules and tie molecule entanglements stretch (Figure 6a) until they can stretch no further (Figure 6b). At the same time the lamellae deform by shear, twinning and martensitic transformations (Figure 6c) and this process will continue with time. Kinloch and Young (Ref. 22) state that plastic deformation can occur in semi crystalline polymers and the deformation of crystallites by dislocation movement has been observed by Peterman and Gleiter (Ref. 23). The work put into this deformation process is high and the associated strain is also large. Eventually however, the lamellae break up into smaller units and are incorporated into a new fibrous morphology oriented approximately parallel to the direction of extension (Figure 6d), leading ultimately to failure. The total amount of deformation is therefore high.

The process whereby brittle failure occurs over long time intervals and at lower stresses is, in its early stages, similar to the ductile deformation process described above. The tie molecules and tie molecule entanglement stretch, but the stress is not sufficiently high to plastically deform or break up the crystallites. The material remains in this state for relatively long periods of time allowing tie molecules to untangle and relax or break by thermally activated processes with little increase in strain. After a finite period of time most of the tie molecules will have disentangled themselves leaving too few to support the load. The material therefore fails at a lower strain than the ductile process described above (Figure 7).

6.2 Environmental Effects

The effect of raising the temperature on 'brittle' failure is to increase the mobility of the tie molecules allowing them to 'untangle' or relax more quickly and thereby lead to shorter times to 'brittle' failure (Figure 4) (Ref. 24).

Brown et al (Ref. 25) note that a service temperature of 20°C is equivalent to approximately 0.7 T_m (the melting temperature) for polyethylene at which the crystallites can move easily in a rubbery amorphous matrix. Under these conditions they suggest that molecular mobility is high and that brittle failure should be expected. Temperature is therefore frequently used as an accelerating factor as described in Section 5.

The process of rupture of tie molecules is essentially chemical in nature (Ref. 21) and is therefore strongly influenced by the presence of anti-oxidant additives or other stabilisers. Gebler (Ref. 15) shows that carbon black imparts a considerable improvement to long term pipe performance and moves the 'knee' to longer times. The material used for Tensar geogrids contains carbon black for UV protection as well as other unspecified antioxidants and stabilisers.

Using the oxidation induction time (OIT) as a measure of stability, Gebler has demonstrated that when antioxidants are present the 'knee' and onset of 'brittle' rupture are associated with the antioxidants being consumed and no longer effective. Beyond this point molecular weight decreases rapidly. He also shows that there is a limit to the amount of

stabiliser which may be added and therefore a limit to the duration to which the knee may be postponed.

Aggressive environments will accelerate rupture, although the precise mechanisms by which they operate are more complex than simple chemical attack. They are believed to 'lubricate' the tie molecules and accelerate unravelling.

Typical environments quoted as being potential promoters of ESC are synthetic detergents, soaps, alcohols, brake fluid, chromic acid, emulsifiers, fatty acids, ethyl alcohol, vegetable and animal oils, oleic acid, palmitic acid, silicone oils, stearic acid and weed killer (Refs. 26, 27).

It should be emphasised however that this data is all based on unoriented grades of polyethylene and that no conclusions concerning the behaviour of oriented grades can be drawn.

6.3 The Effect of Molecular Structure

Lustiger and Rosenberg (Ref. 8) identify the molecular parameters of most relevance to optimising the resistance of polyethylene to slow crack growth.

Molecular weight is clearly of great importance since the higher the molecular weight is the longer are the polymer chains. This results in more tie molecules and more effective tie molecule entanglements. High comonomer content and longer comonomer branches provide better resistance to brittle failure, because those parts of the polymer molecules with long branches do not enter the lamellar lattice and therefore add to the intercrystalline tie molecule material (Figure 8). The short chain branches also act as protrusions inhibiting the ability of the tie molecules to slip over each other (Ref. 28) (Figure 9).

Higher levels of crystallinity leave fewer amorphous intercrystalline tie molecules to hold the crystallites together. Where the orientation of the crystalline lamellae is perpendicular to the tensile stress the material is susceptible to interlaminar failure (brittle). It may be inferred that if oriented parallel to the direction of stress the resistance to brittle failure should be enhanced.

Tie molecules are clearly of great importance to the failure process of polyethylene (Ref. 29). Lustiger and Markham (Ref. 30) liken the tie molecules to 'cement' which holds the lamellar 'bricks' together and state that their integrity is essential for ductile failure to occur. Polyethylene materials which contain relatively few tie molecules are susceptible to the various modes of brittle failure and vice-versa. However, it should be noted that where the ratio of tie molecules to crystalline material is too high the material will exhibit excellent ductility but very much lower stiffness. Since a balance of properties needs to be obtained medium density polyethylenes are frequently selected.

Cross-linking (i.e. chemical bonds between separate molecular chains) provides anchorage points for the chains which restrain excessive movement and maintain the position of the chain in the network. Ifwarson and Erikson (Ref. 21) have shown that cross linking improves the brittle failure resistance of polyethylene by inhibiting intermolecular slip. They

quote typically that 60-70% cross linking is optimal (Grades of polyethylene used for geogrids are not cross linked).

Lustiger et al. (Ref. 24) have shown that potential grades of polyethylene for piping applications can be evaluated by use of constant load tests in a stress cracking environment such as Igepal. They show that the presence of the environment does not change the failure process or the ranking order of different materials but does accelerate the failure process to a time conducive to laboratory investigation perhaps by lubricating the flow of the molecules over each other. They also point out the high susceptibility of failure time to surface imperfections.

Chan and Williams (Ref. 26) also recommend that aggressive environments and elevated temperatures may be used to rank 'tough' polymer materials but that although this is a 'safe' technique it is also a conservative one.

The molecular parameters of most relevance to the delaying of low strain failures of polyethylene are therefore summarised in Table 1.

7. THE STRUCTURE OF DRAWN AND ULTRA HIGH MODULUS POLYETHYLENE

The microstructure of unoriented polyethylene has been described in some detail in Section 6 and can be summarised as a system of randomly oriented crystallites of a lamellar form situated within an amorphous matrix and linked together by 'tie molecules'(or molecular bridges).

The result of extrusion of the polyethylene sheet is to orient the crystallites generally in a direction parallel to that of the applied force.

The process for production of Tensar geogrids involves the heating and drawing of this sheet (punched with a regular pattern of holes) to a draw ratio of approximately 8.5. The process is considered to be cold drawing as the temperature is well below the melting temperature.

Wrigley (Ref. 5) states that the main change to the structure during this process is more extreme molecular orientation. Spherulites are transformed into microfibrils and the crystallites and molecular chains are drawn into alignment, with some crystallites breaking down to form smaller units by chains unfolding rather than chain scission.

This interpretation of the structural changes which occur during manufacture of polyethylene grids is similar to the microstructural explanation of the deformation of unoriented material at high loads (approximately 90% of failure load) and applied relatively quickly. The draw ratio of 8.5 is achieved by the plastic deformation of crystallites as described and by stretching of tie molecule entanglements. However, the process is stopped before failure can occur and the deformed structure 'frozen-in' by cooling. The grid then consists of smaller oriented crystallites linked by elongated tie molecule entanglements and embedded in a slightly oriented amorphous matrix.

This description of a microfibrillar structure agrees well with Peterlin's (Ref. 31) and

Ward's (Ref. 32) earlier interpretations of the molecular structure of highly drawn ultra high modulus fibres and films. Peterlin's description of the structure of these materials is that oriented crystallites are embedded in partially oriented amorphous material and the tie molecules which link the crystallites are almost fully taut. He states that in those materials the tie molecules are the sole candidate for rupture since the rest of the sample is too well protected by packing within the crystal lattice or does not carry load (ie folds and cilia). The failure mechanism is then a coalescence of flaws caused by tie molecule fractures.

Other than Ref. 5, which follows Ward's model for high modulus oriented polyethylene (Refs. 33-35) there is no published information on the microstructure of polyethylene grids. However, ERA considers that bulk unoriented material and highly drawn films and fibres with draw ratios of between 10 and 30 are two extremes and that the structure of the Tensar product, with a draw ratio of 8.5, lies between these and has different additive and copolymer content. Table 2 summarises the microstructural changes in polyethylene during processing.

While there is no exact model for the microstructure of Tensar, the use of Ward's model to interpret creep data indicates the presence of two thermally activated mechanisms. The first, which is responsible for the initial or primary creep, reduces to a logarithmically decreasing strain rate. This mechanism has been associated with deformation of the crystalline regions and is highly dependent on draw ratio. The second process or secondary creep, which takes place at a constant strain rate, only becomes significant when the strain rate due to primary creep has become low enough, leads ultimately to failure and is associated with the deformation and rupture of tie molecules. The explanation of creep by these mechanisms is, however, far from conclusive.

In summary, the ribs of Tensar have a drawn structure but one which permits further deformation of the crystallites and tightening of the tie molecules.

8. OBSERVED STRESS-RUPTURE IN POLYETHYLENE GEOGRIDS

8.1 Available Data

Very few explicit results have been published on the stress-rupture of geogrids. Wrigley (Ref. 5) provides some results on Tensar SR1, an early geogrid formulation, indicating a reduction of strength from approximately 65 to 40% of breaking load between 1 and 10000 h. No information is provided on the strains to failure.

Netlon Ltd have provided a list of data for this study, which is presented in Table 3. It consists of the results of a number of tests on Tensars SR55, 80, 110 and 2 which ended in rupture, and certain other very long-term tests whose durations, in spite of being terminated before rupture, provide a minimum value to the rupture lifetime. Many of the tests were verified by ERA or submitted to and accepted by the British Board of Agrément. They have been augmented by some results of tests on Tensar SR2 conducted at ERA for another client and reproduced with his permission : these tests were carried out over a wider temperature tolerance of 20-23°C but a figure of 20°C has been used for evaluation.

Time to rupture was not always recorded precisely, particularly at long durations. Where the necessary information exists, time to rupture is taken as the mean between the

times to the last occasion on which the specimen was seen unbroken and the occasion on which it was found broken. In some cases either the first, or the second, time was used. In view of the logarithmic scale of the diagrams the effect on the calculations is negligible.

The data are presented as eleven diagrams (four materials, three temperatures except SR2 at 10°C), as load plotted against the logarithm of time (Figures 10-20). In each diagram the times to 10% strain are represented by open circles and linked by straight lines.

8.2 Extrapolation of Time to 10% Strain and Time to Rupture

Since rupture has always been demonstrated to occur at strains exceeding 10% and frequently 15%, Netlon's practice, with the aim of protecting its equipment, is to keep creep test measurements going beyond 10% strain, but to take instruments off test specimens at strains beyond 10% when rupture is imminent or at the end of a test programme. Consequently there is less data on time rupture than on time to 10% strain. Instead of providing extrapolated times to rupture, the times to 10% strain are extrapolated to provide a design limit based on a strain of 10% to 120 years.

This approach has been used in Netlon's report 'Long term sustained load testing of Tensar SR55, SR80, SR110 and SR2 geogrids at a temperature of 40°C \pm 2°C', issued in September 1989 and initialled by ERA.

The difference between extrapolation of times to 10% strain and times to rupture is illustrated by the results of Tensar SR2 at 40°C (Figure 20). It appears that the extrapolated rupture curve may cross the extrapolated times to 10% strain, i.e. that at long time durations rupture may occur at strains below 10%. It is therefore essential to base design loads upon rupture data.

One of the reasons for the reluctance to perform stress-rupture tests is the extent of the effort required. Due to the scatter it is necessary to repeat tests many times to have sufficient confidence to carry out extrapolation (Refs. 36, 37). At least 12 separate tests are recommended in order to define a stress-rupture line over a range of stresses under otherwise identical conditions. Many more tests are required where statistical confidence limits are to be established : work on polyaramid fibres by Glaser et al (Ref. 38) takes confidence limits from 600 data points.

In theory it should be possible to derive further data by calculating the creep curve using the Wilding and Ward theory (Ref. 35). This was proposed by Jewell and Greenwood (Ref. 36). Yeo (Ref. 39) has demonstrated further that the rate of secondary creep is related to the yield behaviour and could therefore be predicted from slow strain rate tensile tests. These methods, however, can only be applied if the strain to failure is constant, but as the above results and also Yeo's very slow strain rate test indicate, this is not the case. The Sherby-Dorn diagrams derived from both Wilding and Ward's and Netlon's creep data indicate that secondary creep is dominant where rupture occurs. As indicated in the last section, secondary creep has been associated with the failure of tie molecules. Extrapolation of the time of inception to secondary creep provides an alternative to the time to 10% strain, but the extrapolation may be non-conservative in the same way if the strain at rupture reduces with time.

8.3 Curve Fitting

The loads in Table 3 were expressed as a fraction of the corresponding mean batch strengths σ_B provided by the manufacturer, determined on single ribs at a crosshead speed of 100 mm/min (50 mm/min for SR2). The results from Tensars SR55, SR80 and SR110 were then superimposed. The purpose of this approach is to obtain more data on a single diagram and thus a more credible extrapolation. Tensars SR55, SR80 and SR110 are made from the same material with an identical method of manufacture, Tensar SR2 was treated separately since although the raw material is the same the hole punched before drawing is of a different shape and this is known to affect the rupture behaviour of the product.

The superimposed points for Tensars SR55, SR80 and SR110 are shown in Figures 21-23 for the three temperatures. There is apparently a satisfactory superposition. Curve fitting was then carried out. Times to 10% strain and to rupture were treated independently. The general relation applied was :

$$\text{double logarithmic} \quad : \quad \sigma = A_0 + A_1 \log(\log 10^x t)$$

The factor of 10^x ($x=1.2$ or 3) has been included in the double logarithmic relation to eliminate decimal values of t . This relation has the benefit of eliminating negative logarithms of which the second logarithm cannot be taken. In each case the coefficients were optimised to minimise the sum of squares of the residual errors. A weighting factor of 0.75 was applied to the contributions from unverified points (marked N/U in Table 3). The choice between the different relations was based upon the calculated goodness of fit (lowest root mean square of residual errors).

The following relations were also considered but were excluded either as being insufficiently accurate or for giving impractical long term extrapolations :

$$\text{linear} \quad : \quad \sigma/\sigma_B = A_0 + A_1 \log t$$

$$\text{parabolic} \quad : \quad \sigma/\sigma_B = A_0 + A_1 \log t + A_2(\log t)^2$$

Time-temperature superposition was then applied by shifting the curves for 20 and 40°C along the time axis to superimpose on that for 10°C and at the same time optimising a new curve to fit the superimposed points. At this stage it became necessary to exclude points exceeding $0.7 \sigma_B$. As σ approaches σ_B the stress-rupture curve should approach the line $\sigma/\sigma_B=1.0$ asymptotically. The double logarithmic model does not include this feature and must therefore be seen as an empirical fit at medium and long durations only.

The resultant curves for 35°C are as follows :

| | | | |
|-----------|---|--------------------|-------------------|
| Figure 24 | : | time to 10% strain | SR55, SR80, SR110 |
| Figure 25 | : | time to rupture | SR55, SR80, SR110 |
| Figure 26 | : | time to 10% strain | SR2 |
| Figure 27 | : | time to rupture | SR2 |

In each diagram the temperatures from which the individual points were derived are marked by separate symbols : for example the pattern of ruptures in Figure 21 can be

recognised (omitting points above 0.7 stress ratio) as full circles in Figure 25. Reference to the grades of Tensar has not been continued beyond Figures 21-23 for the sake of clarity. In all cases the vertical (relative load) axis remains unchanged.

The time shift factors ($\Delta \log t$) can be expressed as a numerical shift on the horizontal scale ($\log t$) where t is the time to rupture in hours. Thus if the temperature is increased by 10°C and the time shift factor is 1.0, the logarithm of time to rupture is reduced by this amount, say from 4.0 to 3.0. Since time is on a logarithmic scale, these shifts can also be regarded as index powers for time; thus in the above example the reduction in lifetime is $10^{-1.0} = 0.1$, and a lifetime of 10000 h is reduced to 1000 h.

The rule for tests terminated without rupture, known as 'run-outs', was as follows. Initially they were excluded and a curve calculated for ruptures alone. If when plotted any 'run-outs' appeared to the right of the curve, they would have been introduced into the calculation and a new curve calculated; if they appeared to the left they were excluded. In the event no 'run-outs' were used in the calculation.

A one-sided 95% confidence limit was added in accordance with the methods given in Ref. 40. It represents a lower boundary such that there is a 95% probability that any subsequent measurement made will lie above this line. Its hyperbolic shape, which allows for a wider limit when extrapolated, reflects the variance of the estimates of slope and mean but does not include the variance of the time-temperature shift (Figure 28). Finally, the shift factor for a temperature of 35°C was interpolated and the resultant curves printed out for a temperature of 35°C .

The results are as follows :

Tensar SR55, SR80 and SR110

Temperature shift formula

$(\Delta \log t)_0 = 0.104599 (\Delta T)_0 - 0.0002033(\Delta T)_0^2$; where $(\Delta T)_0$ is in degrees Celsius measured from 0°C .

Expressed with respect to 35°C ,

$(\Delta \log t)_{35} = 0.090368 (\Delta T)_{35} - 0.0002033 (\Delta T)_{35}^2$;

where $(\Delta T)_{35}$ is the temperature shift in degrees Celsius measured from 35°C

Numerical examples are:

| T ($^{\circ}\text{C}$) | $(\Delta \log t)_0$ | $(\Delta \log t)_{35}$ |
|--------------------------|---------------------|------------------------|
| 0 | 0 | -3.4119 |
| 10 | 1.0257 | -2.3863 |
| 20 | 2.0107 | -1.4013 |
| 25 | 2.4879 | -0.9240 |
| 30 | 2.9550 | -0.4569 |
| 35 | 3.4119 | 0 |
| 40 | 3.8587 | +0.4468 |

The direction of shift is such that a rise in temperature corresponds to more rapid creep.

Time t_{10} to 10% strain at 35°C :

$$\sigma/\sigma_B = 0.5572 - 0.2494 \log(\log 1000t + (\Delta \log t)_{35})$$

One sided 95% confidence limit:

$$\sigma/\sigma_B = 0.5572 - 0.2494 \log(\log 1000t + (\Delta \log t)_{35}) - 0.04037 \downarrow \{1.0233 + [\log(\log 1000t + (\Delta \log t)_{35}) - 0.3485]^2/4.8497\}$$

At 35°C, $t_{10} = 10^6$ h, $\sigma/\sigma_B = 0.3192$, 95% confidence limit = 0.2778

Time to failure t_f at 35°C:

$$\sigma/\sigma_B = 0.6518 - 0.3574 \log(\log 100t + (\Delta \log t)_{35})$$

One sided 95% confidence limit:

$$\sigma/\sigma_B = 0.6518 - 0.3574 \log(\log 100t + (\Delta \log t)_{35}) - 0.03314 \downarrow \{1.0233 + [\log(\log 100t + (\Delta \log t)_{35}) - 0.4188]^2/1.3826\}$$

At 35°C, $t_f = 10^6$ h, $\sigma/\sigma_B = 0.3290$, 95% confidence limit = 0.2927

σ/σ_B for $t_f = 10^6$ h at other temperatures:

The extrapolated rupture loads are:

| | A | B | | B | B | B |
|------------------|---|--------------------|----------------------------|------------------------|------------------------|-------------------------|
| Tempera- ture | σ/σ_B for t_f = 10^6 h | 95% conf. limit | reduction factor A/B | Tensar SR55 kN/m | Tensar SR80 kN/m | Tensar SR110 kN/m |
| 20°C | 0.3589 | 0.3234 | 1.11 | 17.8 | 25.8 | 35.6 |
| 25°C | 0.3481 | 0.3123 | 1.11 | 17.2 | 25.0 | 34.4 |
| 30°C | 0.3382 | 0.3021 | 1.12 | 16.6 | 24.2 | 33.2 |
| 35°C | 0.3290 | 0.2927 | 1.12 | 16.1 | 23.4 | 32.2 |
| 40°C | 0.3206 | 0.2840 | 1.13 | 15.6 | 22.7 | 31.2 |

Note that at 10^6 h, σ/σ_B is higher for failure than for 10% strain, i.e. the predicted strain of failure will exceed 10%.

Tensar SR2

Temperature shift formula

$\Delta \log t = 0.12179 (\Delta T)_0$, where $(\Delta T)_0$ is the temperature shift in degrees Celsius measured from 0°C.

| T (°C) | ($\Delta \log t$) ₀ | ($\Delta \log t$) ₃₅ |
|--------|----------------------------------|-----------------------------------|
| 0 | 0 | -4.2627 |
| 10 | 1.2179 | -3.0448 |
| 20 | 2.4358 | -1.8269 |
| 25 | 3.0448 | -1.2179 |
| 30 | 3.6537 | -0.6090 |
| 35 | 4.2627 | 0 |
| 40 | 4.8716 | +0.6090 |

Time t_{10} to 10% strain at 35°C:

$$\sigma/\sigma_B = 0.5080 - 0.1985 \log(\log 1000t + (\Delta \log t)_{35})$$

One-sided 95% confidence limit:

$$\sigma/\sigma_B = 0.5080 - 0.1985 \log(\log 1000t + (\Delta \log t)_{35}) - 0.01632 \downarrow \{1.1111 + [\log(\log 1000t + (\Delta \log t)_{35}) - 0.5046]^2/0.8842\}$$

At 35°C, $t_{10} = 10^6$ h, $\sigma/\sigma_B = 0.3186$, 95% confidence limit = 0.2997

Time to failure at 35°C:

$$\sigma/\sigma_B = 0.5123 - 0.2307 \log(\log 10t + (\Delta \log t)_{35})$$

One-sided 95% confidence limit:

$$\sigma/\sigma_B = 0.5123 - 0.2307 \log(\log 10t + (\Delta \log t)_{35}) - 0.04286 \downarrow \{1.2000 + [\log(\log 1000t + (\Delta \log t)_{35}) - 0.2962]^2/0.3520\}$$

At 35°C, $t_f = 10^6$ h, $\sigma/\sigma_B = 0.3173$, 95% confidence limit = 0.2558

σ/σ_B for $t_f = 10^6$ h at other temperature:

Note that at 10^6 h, σ/σ_B is lower for failure than for 10% strain, i.e. the predicted strain at failure is less than 10%.

| Temperature | A σ/σ_B for $t_f = 10^6$ h | B 95% conf. limit | reduction factor A/B | B Tensar SR2 kN/m |
|-------------|--|----------------------|----------------------------|-------------------------|
| 20°C | 0.3476 | 0.2918 | 1.19 | 23.3 |
| 25°C | 0.3364 | 0.2786 | 1.21 | 22.3 |
| 30°C | 0.3265 | 0.2668 | 1.22 | 21.3 |
| 35°C | 0.3173 | 0.2558 | 1.24 | 20.5 |
| 40°C | 0.3090 | 0.2457 | 1.26 | 19.7 |

8.4 Comments on the Calculations

Visually, the stress-rupture diagrams for the three materials appear to superimpose satisfactorily at each temperature. The functions for curve fitting are the most simple to give a satisfactory approximation. As indicated above, the double logarithmic function used is not representative at the highest loads and shortest times.

The temperature shifts were evaluated jointly for the times to 10% strain and the times to rupture, but separately for the two groups of material. For Tensars SR55, SR80 and SR110 a quadratic relation between temperature and logarithm of time was adopted. For Tensar SR2, with only two temperatures, a linear interpolation was made. For Tensars SR55, SR80 and SR110 the mean shift between 10 and 20°C was 0.10/°C and between 10 and 40°C 0.09/°C. For Tensar SR2 the figure was 0.12/°C. Bush (Ref. 41) found a shift of 0.13/°C for the time to 10% strain of Tensar SR55 between 10 and 20°C and 0.15/°C between 10 and 40°C.

The long-term design loads are based on the characteristic strengths guaranteed by the manufacturer. These are lower bound values for the batch strengths σ_B in Table 3 used to derive the ratio σ/σ_B .

The level of scatter has been expressed as a confidence limit in the direction of load. It would be statistically more correct to carry out the analysis in the direction of time rather than stress, but this approach led to mathematical difficulties that could not be resolved within the scope of this project.

Time-temperature superposition is an established method of extrapolating modulus and rupture data for polymers, a short critique of which is given by Turner (Ref. 42). He emphasises the importance of detecting any change in slope arising from a change in mechanism which then invalidates the method. A more detailed description is given in Ref. 3.

8.5 Evidence of 'Brittle' Failure

In ERA's tests on SR2 material there was one notable result where a specimen tested at 40% of the short-term breaking load ruptured after only 11374 h and at a strain of 10.7%. A crack started from the outer edge of the outer rib and led rapidly to failure of the rib. Because of the distortion of the specimen, the local strain at failure was probably higher and the surface was no different from those of specimens that failed at higher strains.

Netlon Ltd suggest that this failure was caused by damage at the rib surface during specimen preparation. Duplicating the test on a specimen taken from the same batch of material under identical conditions in their laboratory, they demonstrated that the creep behaviour was the same but that the specimen survived to 15191 h without rupture at a strain of 10.38%. Netlon then chose to increase the load at intervals up to a level of 45 kN/m in order to fail the sample. The specimen finally ruptured after 17008 hours at a load of 45 kN/m and Netlon claim that the failure strain of 15.86% is within the normal range of failure of SR2 under creep conditions and hence failed in the standard mode. A supplementary test at ERA has lasted 16757 h (at 31.12.90) without failure.

The early failure at ERA could have been due to damage caused during specimen preparation. This may have taken the form of a nick or surface abrasion but in either case represents significant sensitivity of rupture lifetime to site induced damage effects. It is also possible that failure could have been initiated at an agglomerate of carbon black particles as was observed by Peggs and Carlson (Ref. 43) in unoriented geomembranes. Either way, ERA accepts the validity of all three results.

Netlon's subsequent process of inducing ductile failure by increasing the load does not contradict this. If one considers the description of the failure process in polyethylene as put forward by Lustiger and Rosenberg (Ref. 8) and Netlon's own description (Refs. 44, 45) of the molecular structure of the grid it can be deduced that in the early stages of testing of this SR2 specimen the load is of insufficient size to cause any further deformation of the crystallites. The creep load therefore stretches the tie molecules and over a period of time allows them to untangle and relax with the ultimate possibility of failure of the remaining entanglements in a 'brittle' manner.

In increasing the load in increments however to 58% of the short-term breaking load it is possible that Netlon have caused further deformation to the crystallites which as stated in Section 6 results in a higher deformation at failure.

In conclusion, therefore, the evidence for Tensar SR2 indicates that although rupture has been observed to occur at strains well above 10%, when extrapolated to durations of 10^6 hours (114 years) or beyond, failure may occur at strains marginally below 10% strain. A single result suggests the possibility of more brittle failure or alternatively a sensitivity to site induced damage, for which there is a safety factor f_d (see Section 9.2).

8.6 Fractures in the 'Node' Areas

ERA has occasionally observed fractures where a split in a Tensar rib under load has propagated into the 'node' areas. When this happens the appearance of failure in the 'node' is quite unlike that in the ribs : it is granular, with limited evidence of ductility, occurring diagonally or transverse to the ribs. The material in this area is only lightly drawn (draw ratio approximately 1.5) and it is suggested that this is the 'brittle' rupture of unoriented polyethylene. It is significant that, even with the presence of a stress raiser, such fracture has not been observed in the ribs but only in the nodes.

8.7 Is There a 'Knee' in the Rupture of Geogrids?

In the last section it was shown on the basis of the evidence available that the slopes of the stress-rupture graph in geogrids appear to be slightly steeper than the isometric curves, indicating that rupture takes place at progressively lower strains. Such curves can be extrapolated to provide design loads, although extrapolation over such long times on the basis of so few points is not recommended. Extrapolation assumes, however, that in geogrids there is no 'knee' in the curve such as that which occurs in unoriented polyethylene. There is no direct evidence for such a knee and the arguments for and against its existence are therefore circumstantial.

Netlon's own opinion on the possibility of a knee in the stress-rupture curve has been put forward by Wrigley (Refs. 44, 45). He argues that the elevated temperature drawing will stretch the tie molecules and break up and orient the crystallites to form a fibrous, oriented morphology in a manner analogous to that described in Section 6 (Ref. 30). Cooling of the drawn structure 'freezes in' this molecular morphology. According to Wrigley therefore, it follows that all potential for the 'ductile' type of failure has been removed by the fabrication process which has already taken the material through the ductile failure mechanism (such as twinning, dislocation movement and breaking of lamellae). All failures of the finished product under long-term loading therefore will be brittle in nature being a consequence of the disentanglement and failure of tie molecules under load. Wrigley further points out that although referred to as 'brittle' failure the extension at failure is still of the order of 15 to 20%.

Some supportive evidence can be drawn from the work of Ward et al (Ref. 46) who measured stress-rupture curves for polyethylene pipes of different grades (homopolymer and copolymer) and obtained by different fabrication routes. Some of these pipes had been produced by normal methods while others had been die-drawn to a draw ratio of approximately 9 at a temperature similar to that used in the Tensar fabrication process. It was found that in all cases the failure of die drawn pipe was brittle and the authors suggest that there is no possibility of a change in failure mode at longer times and lower stresses.

However, the results they present do show a knee in the stress-rupture curve for die drawn homopolymer pipe inferring that the improvements are only seen where the base material is copolymer. It should also be noted that the data for die drawn copolymer pipe are not entirely conclusive since they do not extend to long enough test periods.

For unoriented material it has been shown that the ductile to brittle transition zone of the stress-rupture curve (i.e. the knee) corresponds to a change in the failure mechanism; to the left of the knee the loads are high enough to cause failure in a relatively short time by extension of tie molecules and plastic deformation of crystallites, resulting in high failure strains. To the right of the knee the load levels are sufficient only to extend the tie molecules and not to deform the crystallites; failure in this case occurs by the gradual unravelling of tie molecule entanglements and failure of individual tie molecules all of which result in low strains and longer times to failure. It can be deduced from this that where there is scope for further deformation of the crystalline fraction of the material as well as extension of the tie molecules there must also be scope for a change in failure mechanism dependent on the applied load. If the observed ruptures have a 'ductile' component the potential exists for a more 'brittle' failure and therefore a knee.

In support of this argument it should be noted that the gradients of the stress-rupture curves for Tensar SR2 at 40°C and 23°C when plotted on a double logarithmic scale are approximately -1/20 and -1/16 which are similar to those observed in the ductile region of the stress-rupture curve of unoriented polyethylene. It is therefore possible that the 'knee' exists, but has been displaced to long durations.

The various modifications to the polymer in molecular weight, additive content and degree of copolymerisation have been undertaken in part to delay the onset of the brittle failure mode. This has been the case for material grades used in gas and water distribution networks and therefore by choosing a pipe grade material for the Tensar geogrids, Netlon

have ensured that environmental stability and resistance to brittle type failure modes are as good as possible. Netlon's own creep tests on SR80 material run to approximately 20000 h at 31.3 kN/m at 20°C (strain : 9.3%) and have exceeded 30000 h at several loads at 10°C (e.g. strain 10.3% after 34416 h at 35.8 kN/m, see Table 3).

Any argument for a 'knee' must therefore concede that in Tensar it has been postponed to very long durations. Against it, however, stands the evidence of the creep tests that the stress-ruptures observed are already in the region of 'secondary creep' which is associated with the rupture of tie molecules. In addition, microscopic evidence suggests that the 'brittle' failure of unoriented polyethylene only occurs in the lightly drawn areas and only when introduced by a stress raiser.

We therefore suggest that there is no knee in the stress-rupture behaviour of Tensar ribs and that there is a single failure type for geogrids. This judgement is, however, based on limited evidence and work is urgently needed to substantiate it further. One method of doing this would be to accelerate it.

Stress-rupture testing in an ESC (Environmental Stress Cracking) environment has been shown to accelerate the occurrence of brittle failure modes and is suggested as a method of observing the existence of such transition zones, and ranking a material's susceptibility to ESC.

Two similar detergents commonly used to promote environmental stress cracking are Comprox (BP Detergents Ltd) (2% solution) and Igepal. Both solutions have been shown to accelerate the occurrence of brittle failure. Reference 24 concludes that this is on account of enhanced molecular movement.

BP Chemicals carried out a series of ESC tests on samples of the early product Tensar SR1 on behalf of Netlon Ltd. The environment chosen was 2% Comprox solution at 23°C. This surfactant solution has been used by other researchers (Refs. 24 & 26) for promoting environmental stress cracking in unoriented grades of polyethylene. Loads were selected to bring about failure within 0.1 to 2000 hours was expected to be sufficient to demonstrate any difference. The results show no difference between the stress-rupture curves tested in air or surfactant and consequently Netlon conclude that Tensar grids are unaffected by ESC.

ERA agrees with the choice of 23°C to be relevant to the UK soil environment but notes that other workers (Refs. 24 & 26) have raised the solution temperature solely for the purpose of accelerating any ESC effects. The argument against ESC in geogrids would be strengthened if the temperature were raised thereby providing data on what may happen to an ambient test over much longer periods of time than those examined. It should be noted that the data presented in Ref. 5 is the only available evidence on ESC of drawn (oriented) HDPE geogrids; no conclusions can be drawn from work on unoriented PE and there is an identifiable requirement for results to be generated. Reference 46 emphasises the variability in behaviour between different grades of HDPE.

There are two interconnected areas of concern, however. The first is the vulnerability of the nodes to brittle fracture if a stress-raiser is introduced by means of a split rib or site damage. As Whelton and Wrigley point out, the material at the nodes may be more susceptible both to environmental stress cracking and brittle fracture although the stress here

is considerably lower (Ref. 47). Particular attention should therefore be paid to the effects of stress concentrators in these regions.

Secondly, if premature failure mentioned earlier is due to abrasion or induced damage, then it indicates a high sensitivity to local damage in the ribs as well as the nodes. Safety factors recommended by Netlon for the effects of damage vary from 1.05 to 1.70 and are based on the reduction in short-term breaking load (ductile failure). It is possible that the effect on the stress-rupture behaviour may be more severe, although creep tests at ERA on notched material have so far not indicated a further embrittlement due to a stress raiser. However, long-term rupture tests on abraded material should be carried out for verification of the safety factors.

9. RECOMMENDATIONS FOR DESIGN PROCEDURES

9.1 Design Loads

The design loads are for Tensar geogrids. They are based on characteristic batch strengths extrapolated to 10⁶h usage.

| Temperature | Tensar SR55 kN/m | Tensar SR80 kN/m | Tensar SR110 kN/m | Tensar SR2 kN/m |
|-------------|------------------------|------------------------|-------------------------|-----------------------|
| 20°C | 17.8 | 25.8 | 35.6 | 23.3 |
| 25°C | 17.2 | 25.0 | 34.4 | 22.3 |
| 30°C | 16.6 | 24.2 | 33.2 | 21.3 |
| 35°C | 16.1 | 23.4 | 32.2 | 20.5 |
| 40°C | 15.6 | 22.7 | 31.2 | 19.7 |

9.2 Safety Factors

9.2.1 General

The safety factors to be applied to geotextiles for use in soil reinforcement are the product of the following partial safety factors (Ref. 36), see Figure 29.

| | |
|-----------|---|
| f_m | material factor |
| f_d | installation damage |
| f_{env} | chemical and biological degradation (excluding synergy with load) |
| f_c | inaccuracies in design of structure |

Not all of these will necessarily be included, since some may be regarded as of insignificant risk, and it is important to eliminate any duplication.

In this analysis we are concerned with f_m alone. This should take into account a number of contributory factors described in the following :

9.2.2 Scatter of Extrapolation, Uncertainty in the Method of Extrapolation

The calculations of Section 8.3 for Tensar materials indicate reduction factors (to 95 % confidence limits for a lifetime of 10^6 h) of between 1.11 and 1.13 for SR55, 80 and 110 (1.19 to 1.26 for SR2). The level of scatter has been measured and referred to mean strength; in calculating the load levels, however, nominal characteristic strengths rather than mean values of strength have been used. The lower value of the scatter band is thus conservative.

As described above, the scatter assumes a double logarithmic relation. Although this appears to give a reasonable fit, application of different curve-fitting laws will, when extrapolated, lead to different predictions. The choice between extrapolation laws is subjective.

The longest measured times to rupture are :

| | |
|------|--------|
| 10°C | 4536 h |
| 20°C | 8400 h |
| 40°C | 1849 h |

and it is recommended that a contributory safety factor exceeding unity should be applied where the design lifetime exceeds ten times these lifetimes (i.e. one log cycle of time), in particular for a design lifetime of 10^6 h or 120 years.

9.2.3 Synergy between Load and Damage Effects

Netlon recommends separate safety factors f_d for use with fine and coarse fills, based on the measured reduction in short-term tensile strength (Ref. 49). The method of applying these strain data is conservative. There is an additional possibility that the reduction in long-term strength is greater than the reduction in short term strength. The result on Tensar SR2 described in Section 8.5 is an indication of this. A contributory safety factor is proposed.

9.2.4 Environmental Stress Cracking (Synergy between Load and Environmental Effects)

While the safety factor f_{env} covers the direct effect of chemical environments, it is well known that materials under load are more sensitive to chemical attack, the effect being known as environmental stress cracking (ESC). This is in effect a synergy between load and environmental effects. It is argued however in Section 8.7 that Tensar is insensitive to ESC, so that no safety factor is recommended.

9.2.5 Possible Change in Rupture Mechanism

This is described at length in Section 8.7 where it is concluded that a transition is unlikely. There remains, however, an element of uncertainty, giving a small probability of a main reduction in lifetime. A contributory factor therefore is recommended.

9.2.6 Effects of Temperature Greater than 35°C

The time-temperature superposition indicates shifts of between 0.089 and 0.122 on a logarithmic timescale per degree change in temperature, amounting to multiplication factors of 1.22 to 1.32 per degree celsius. The soil temperatures in Hong Kong are described in Ref.50, where it is shown that in a location 13 mm below the surface of a concrete slab the summer temperature frequently exceeds 40°C. Taking a less extreme case, one could consider as an example that the temperature in the reinforcement with a concrete cover would reach 40°C for a total of 180 h per year. Even when multiplied by a timeshift factor of 4.06 ($10^{0.609}$) corresponding to the difference of 5°C for Tensar SR2, the change in 'lifetime' is only 8.3% of a year. Since the level of 35°C is relatively conservative, for most soil reinforcements a contributory safety factor to take into account excesses in temperature would appear unnecessary.

Comparable statements can be made for lower design temperatures. Assessment of the safety factor will, however, depend on the engineer's own estimate of the likelihood of his design temperature being exceeded.

9.2.7 Dynamic Loading

There is no experimental data on dynamic fatigue on Tensar. Dynamic fatigue, resulting in gradual defibrillation, is known in linearly oriented textile fibres. While no safety factor is proposed for normal reinforcement applications, it is recommended that where dynamic loads, due for example, to road traffic, are significant, special performance tests should be carried out to determine the design load.

9.2.8 Probability of the Material Strength being less than its Characteristic Value

The calculations above are based on a one-side 95 % confidence limit, i.e. one specimen in 20 falls below the lower limit of ratio of rupture strength to batch tensile strength. The long-term stress-rupture loads are then calculated using the manufacturer's characteristic strength and his quality assurance scheme ensures that any batch with a lower measured tensile strength is rejected at the quality control stage. The introduction of a safety factor will depend upon whether these safeguards are regarded as sufficient.

9.2.9 Dimensional Effects on Strength

This factor reflects the sensitivity of the material to small defects, in particular the tendency of a textile to tear, reflected by a sensitivity of tensile strength to specimen size. This is similar to the notch sensitivity of brittle solids. Such an effect is unlikely to occur in the relatively ductile geogrids and Netlon has indicated that specimens of different widths have similar strengths. No safety factor is recommended.

The values of these safety factors must be determined for each individual product and application.

10. CONCLUSIONS

Extrapolation of the stress-rupture data on drawn (oriented) HDPE geogrids to 10^6 hours (approximately 120 years) at 35°C leads to the following design loads for four products :

| Temperature | Tensar SR55 kN/m | Tensar SR80 kN/m | Tensar SR110 kN/m | Tensar SR2 kN/m |
|--------------------|------------------------|------------------------|-------------------------|-----------------------|
| 20°C | 17.8 | 25.8 | 35.6 | 23.3 |
| 25°C | 17.2 | 25.0 | 34.4 | 22.3 |
| 30°C | 16.6 | 24.2 | 33.2 | 21.3 |
| 35°C | 16.1 | 23.4 | 32.2 | 20.5 |
| 40°C | 15.6 | 22.7 | 31.2 | 19.7 |

In Tensar SR2 it is predicted that at 10^6h rupture may occur at less than 10% strain. The design loads based on extrapolation of time to 10% strain are therefore too high. In the remaining products the strain at rupture at 10^6h is predicted to exceed 10%.

In unoriented pipe grade HDPE there are two rupture mechanisms. At high loads and short times rupture is ductile and the stress-rupture graph extrapolates to long rupture lifetimes. At lower loads and longer time intervals, however, there is a transition to more brittle failure (strain to failure 5 to 35%), leading to reduction in extrapolated lifetime. This transition or 'knee' exists for any grade of unoriented material. In Tensar geogrids there appears to be only one mode of rupture : it occurs in the ribs at strains similar to the 'brittle' failure of unoriented polyethylene, but it is not possible to state that the two processes are the same. On the available evidence it is proposed that there is no 'knee' in the stress-rupture graph of Tensar geogrids, although with the limited evidence available a partial safety factor is recommended.

The contributions to the safety factor f_m have been reviewed. These include :

- (a) scatter of extrapolation; uncertainty in the method of extrapolation,
- (b) synergy between load and damage effects,
- (c) environmental stress cracking,
- (d) possibility in the change of rupture mechanism,
- (e) effect of temperature greater than 35°C ,
- (f) dynamic loading,
- (g) probability of the material strength being less than its

characteristic value, and

(h) dimensional effects on strength.

An extensive review of the literature has shown that there are no other data available for the stress-rupture of drawn HDPE geogrids. While the methodology and the considerations concerning the contributions to f_m could be applied to any other product, the numerical results and the argument concerning the occurrence of brittle failure are peculiar to the Tensar products described in this report.

11. RECOMMENDATIONS FOR FURTHER WORK

Confirmation of the predictions made in this report should be made to establish confidence in the method and to check that there is no transition to any other type of failure mechanism. Tests should also be carried out on damaged geogrids to establish a safety factor based on long-term rupture lifetime rather than short-term strength. These tests will enable the safety factors to be modified. All tests, including stress-rupture tests over a range of loads and temperatures, in selected chemical environments, and following damage by different fill materials, will be necessary for other types of HDPE geogrid.

12. REFERENCES

1. Billmeyer, F.W. *Textbook of Polymer Science. (Second Edition)*. Wiley-Interscience, New York, 1971, ISBN 0471072966, 597 p.
2. Keller, A. A note on single crystals in polymers : evidence for a folded chain configuration. *Philosophical Magazine, (Eighth Ser.)* vol. 2, Sep 1957, pp 1171-1175.
3. Ward, I.M. *Mechanical Properties of Solid Polymers. (Second Edition)*. Wiley-Interscience, Chichester, 1983, ISBN 0471900117, 471 p.
4. Keith, H.D., Padden, F.J. & Vadimsky, R.G. Intercrystalline links : critical valuation. *Journal of Applied Physics*, vol. 42, no. 12, Nov 1971, pp 4585-4592.
5. Wrigley, N.E. Durability and long term performance of Tensar polymer grids for soil reinforcement. *Materials Science and Technology*, vol. 3, Mar 1987, pp 161-170.
6. Hin, T.S. & Chen, B.W. Creep rupture of a linear polyethylene : Paper 1 : rupture and pre-rupture phenomena. *Polymer*, vol. 25, 1984, pp 747-734.
7. Crossman, J.H. & Zappas, L.J. Creep failure and fracture of polyethylene in uniaxial extension. *Polymer Engineering and Science*, vol. 19, 1979, pp 99-103.
8. Lustiger, A. & Rosenberg, J. Predicting the service life of polyethylene in engineering applications. *Seminar on Durability and Ageing of Geosynthetics*, Drexel University, Philadelphia, 1988, Paper no. 13.

9. Eriksson, P. & Ifwarson, M. Occurrence of brittle fracture in polyethylene. *Kunststoffe German Plastics*, vol. 76, no. 6, Jun 1986, pp 512-516.
10. Broutman, L.J. How to minimise stress cracking in plastics. *Materials in Design Engineering*, 1965, pp 116-120.
11. Ewing, L. British Gas polyethylene distribution systems. *Pipetech 84*, National Exhibition Centre, Birmingham 1984.
12. Greig, J.M. Specification and testing of polyethylene gas distribution systems for a minimum 50 year operational life. *Plastics and Rubber Processing and Applications*, vol. 1, no. 1, 1981, pp 43-49.
13. Diedrich, G., Kempe, B. & Graf, K. Creep rupture strength of polyethylene (HDPE) and polypropylene (PP) pipes in the presence of various chemicals. *Kunststoffe German Plastics*, vol. 69, no. 8, Aug 1979, pp 18-20.
14. Ifwarson, M. Lifetime of polyethylene pipes under pressure and exposure to high temperatures. *Kunststoffe German Plastics*, vol. 79, no. 6, Jun 1989, pp 525-529.
15. Gebler, H. Long-term behaviour and ageing of PE-HD pipes. *Kunststoffe German Plastics*, vol. 79, no. 9, Sep 1989, pp 823-826.
16. Fleißer, M. Slow crack growth and creep rupture strength of polyethylene pipe. *Kunststoffe German Plastics*, vol. 77, no. 1, Jan 1987, pp 45-50.
17. Gaube, E. & Kausch, H.H. Bruchtheorien bei der Industriellen Anwendung von Thermoplasten und glasfaserverstärkten Kunststoffen. *Kunststoffe German Plastics*, vol. 63, no. 6, Jun 1973, pp 391-397.
18. Gaube, E., Gebler, H., Müller, W. & Gondro, C. Creep rupture strength and ageing of HDPE pipes. *Kunststoffe German Plastics*, vol. 75, no. 7, Jul 1985, pp 12-14.
19. Janson, L.E. *Plastic Pipe in Sanitary Engineering*. Collaborative work between the author and a number of plastics industries, including Granges Essem Plant, Celanese Plastics Company, Newark NJ USA. Published by Granges Essen Plant, Uplands Väsby, Sweden, 1973, 154 p.
20. Sandilands, G.J. & Bowman, J. An examination of the role of flaw size and material toughness in the brittle fracture of polyethylene pipes. *Journal of Materials Science*, vol. 21, 1986, pp 2881-2888.
21. Ifwarson, M. & Eriksson, P. Experience from 12 years evaluation of cross linked polyethylene. 6th International Conference on Plastics Pipes, *Plastics and Rubber Institute*, York, 26-28 Mar 1985, Paper no. 40, pp 40A/1-11.
22. Kinloch, A.J. & Young, R.J. *Fracture Behaviour of Polymers*. Applied Science Publishers, London, 1983, ISBN 0853341869, 496 p.

23. Peterman, J. & Gleiter, H. Plastic deformation of polyethylene crystals by dislocation motion. *Journal of Materials Science*, vol. 8, 1973, pp 673-675.
24. Lustiger, A., Markham, R.L. & Cassady, M.J. Environmental stress cracking as a tool for evaluating polyethylene piping materials. *5th International Conference on Plastics Pipes*, Plastics and Rubber Institute, York, Sep 1982, Paper no. 23, pp 23.1-23.8.
25. Brown, N., Donofrio, J. & Lu, X. The transition between ductile and slow-crack-growth failure in polyethylene. *Polymer*, vol. 28, Jul 1987, pp 1326-1330.
26. Chan, M.K.V. & Williams, J.G. Crack growth in high density polyethylenes. *Polymer*, vol. 24, Feb 1983, pp 234-244.
27. BP Technigram T19/1. *Chemical Resistance of Rigidex High Density Polyethylene*. BP Chemicals Ltd, Grangemouth.
28. Lustiger, A. & Markham, R.L. Optimising the resistance of polyethylene to slow crack growth. *6th International Conference on Plastics Pipes*, Plastics and Rubber Institute, York, 26-28 Mar 1985, Paper no. 23, pp 26-28.
29. Brown, N. & Ward, I.H. The influence of morphology and molecular weight on ductile-brittle transitions in linear polyethylene. *Journal of Materials Science*, vol. 18, 1983, pp 1405-1420.
30. Lustiger, A. & Markham, R.L. Importance of tie molecules in preventing polyethylene fracture under long term loading conditions. *Polymer*, vol. 24, Dec 1983, pp 1647-1654.
31. Peterlin, A. Fracture mechanism of drawn oriented crystalline polymers. *Journal of Macromol, Science and B-Physics*, vol. 7, no. 4, pp 705-727.
32. Ward, I.M. The orientation of polymers to produce high performance materials. *Symposium on Polymer Grid Reinforcement in Civil Engineering*, the Institution of Civil Engineers, 1984, Paper 1.1
33. Wilding, M.A. & Ward, I.M. Routes to improved creep behaviour in drawn linear polyethylene. *Plastics and Rubber Processing and Applications*, vol. 1, 1981, pp 167-172.
34. Ward, I.M. & Wilding, M.A. Creep behaviour of ultra high-modulus polyethylene : Influence of draw ratio and polymer composition. *Journal of Polymer Science : Polymers Physics Edition*, vol. 22, 1984, pp 361-375.
35. Wilding, M.A. & Ward, I.M. Creep and stress-relaxation in ultra high modulus linear polyethylene. *Journal of Materials Science*, vol. 19, 1984, pp 629-636.
36. Jewell, R.A. & Greenwood, J.H. Long term strength and safety in steep soil slopes reinforced by polymer materials. *Geotextiles and Geomembranes*, vol. 7, nos 1 & 2, 1988, pp 81-118.

37. Greenwood, J.H., Jewell, R.A. Strength and safety : the use of mechanical property data. *Reinforced Embankments, Theory and Practice*. (Edited by Shercliff D.A.). Thomas Telford London, 1990, pp 83-98.
38. Glaser, R.E., Moore, R.L. & Chiao, T.T. Life estimation of aramid/epoxy composites under sustained tension. *Composite Technology Review*, vol. 6, no. 2, 1984, pp 26-35.
39. Yeo, K.C. The behaviour of polymeric grids used for soil reinforcements. *PhD Thesis, University of Strathclyde*, 1985.
40. ASTM. Manual on fitting straight lines. *Special Technical Publication no. 313, ASTM*, Philadelphia, 1962.
41. Bush, D.I. Variation of long-term design strength of geosynthetics in temperatures up to 40°C. *4th International Conference on Geotextiles and Geomembranes*, the Hague, 1990, Rotterdam : Balkema, pp 673-676.
42. Turner, S. *Mechanical testing of plastics*. (Second edition). Harlow : George Godwin, 1983, pp 85-88.
43. Peggs, I.D. & Carlson, D.S. Stress cracking of polyethylene geomembranes : field experience. *ASTM Symposium on the Microstructure and Performance of Geosynthetics*, Philadelphia, Jan 1989.
44. Wrigley, N.E. The failure mode of 'Tensar' high density polyethylene geogrids. *Abstracted note from a verbal presentation made to Conference on 'Durability and Ageing of Geosynthetics'*, Drexel University, Philadelphia, 1988.
45. Wrigley, N.E. The durability and ageing of geogrids. *Seminar on Durability and Ageing of Geosynthetics*, Drexel University, Philadelphia, 1988, Paper no. 8.
46. Ward, I.M., Selwood, A., Parsons, B. & Gray, A. The production and properties of die drawn PE pipe. *6th International Conference on Plastics Pipes*, Plastics and Rubber Institute, York, 26-28 Mar 1985, Paper no. 2, pp 2.1-2.6
47. Capaccio, G. Comment on paper by Ingold T.S. and Miller K.S. *3rd International Conference on Geotextiles*, Vienna, 1986, International Geotextile Society, pp 1482-1484.
48. Whelton, W.S. & Wrigley, N.E. Long term ductility of geosynthetics soil reinforcement. *Geosynthetics '87 Conference*, New Orleans, LA, Feb 1987, vol. 2.
49. Bush, D.I. Evaluation of the effects of construction activities on the physical properties of polymeric soil reinforcing elements. *Theory and Practice of Earth Reinforcement*, (Edited by Yamanouchi T., Miura N. and Ochiai H., Balkema), 1988, Rotterdam, pp 63-68.

50. Howells, D.J. & Pang, P.L.R. Temperature considerations in the design of geosynthetic reinforced fill structures in hot climates. *Symposium on the Application of Geosynthetic and Geofibre in Southeast Asia*, 1-2 August 1989, Petaling Jaya, Selangor Darul Ehsan, Malaysia, pp 1-1 to 1-7.

LIST OF TABLES

| Table No. | | Page No. |
|--------------|---|-------------|
| 1 | Parameters which Delay or Accelerate the Occurrence of Low Strain Failures in Polyethylene | 35 |
| 2 | Microstructural Changes in Polyethylene during Processing | 35 |
| 3 | Stress-rupture Data for Tensar Geogrids | 36 |

Table 1 - Parameters which Delay or Accelerate the Occurrence of Low Strain Failures in Polyethylene

| Parameter | Effect |
|-------------------|---|
| Molecular weight | Increasing molecular weight increases molecular length and enhances tie molecule entanglement |
| Comonomer content | Higher comonomer content creates more branches and more material which is not part of the lamellar lattice thereby adding to intercrystalline molecular entanglements |
| Crystallinity | Too high levels of crystallinity can reduce the amount of intercrystalline molecular entanglements and reduce resistance to low strain failures |
| Cross linking | Cross linking inhibits intermolecular slip and improves low strain failure resistance |
| Orientation | Orientation of lamellae perpendicular to the applied stress reduces the resistance to brittle failure modes |

Table 2 - Microstructural Changes in Polyethylene during Processing

| Polymer Form | Proposed Microstructure |
|-------------------------------------|---|
| Unoriented cast polymer | Randomly oriented crystallites in an amorphous matrix linked by tie molecules |
| Extruded sheet | Crystallites oriented parallel to the direction of extrusion in an amorphous matrix linked by tie molecules |
| Drawn sheet at elevated temperature | Crystallites broken down by twinning, martensitic transformation etc in a partially oriented amorphous matrix linked by tie molecules which have been elongated in draw direction |
| Highly drawn film and fibres | Highly oriented 'fine' crystallites in partially oriented amorphous matrix linked by 'taut' tie molecules |

Table 3 - Stress-rupture Data for Tensar Geogrids (Sheet 1 of 2)

| Type | Temperature °C | Load kN/m | Mean batch strength kN/m | Time to 10% strain h | Time to failure h | Source and verification | Last measured strain | |
|------|-------------------|-----------|-----------------------------|----------------------------|----------------------|----------------------------|--|--|
| | | | | | | | Time h | Strain % |
| SR55 | 10 | 44.0 | 61.9 | 0.167 | 4.4 | N/U | 16970 | 14.1 |
| | | 38.5 | | 0.639 | 47 | N/U | | |
| | | 33.0 | | 8.4 | 1112 | N/U | | |
| | | 28.35 | | 60 | T | N/BBA | | |
| SR55 | 20 | 44.0 | 61.9 | 0.0032 | 0.68 | N/U | 3523 16970 | 16.7 11.3 |
| | | 38.5 | | 0.075 | 4.3 | N/U | | |
| | | 33.0 | | 0.95 | 112 | N/U | | |
| | | 28.35 | | 2.5 | 3523 | N/BBA | | |
| SR55 | 40 | 44.0 | 61.9 | 0.002 | 0.007 | N/U | 70 2205 8807 | 12.3 12.0 10.3 |
| | | 38.5 | | 0.003 | 0.06 | N/U | | |
| | | 33.0 | | 0.013 | 0.62 | N/U | | |
| | | 24.2 | | 1.58 | T | N/ERA | | |
| SR80 | 10 | 44.0 | 86.9 | 0.002 | 0.007 | N/U | 16 7.3 311 800 4440 34416 | 17.6 12.0 20.5 17.5 13.8 10.3 |
| | | 38.5 | | 0.003 | 0.06 | N/U | | |
| | | 33.0 | | 0.013 | 0.62 | N/U | | |
| | | 24.2 | | 1.58 | T | N/ERA | | |
| SR80 | 20 | 44.0 | 86.9 | 0.002 | 0.007 | N/U | 75.5 75.4 773 3528 8326 24526 | 18.0 19.1 14.8 14.5 12.6 9.6 |
| | | 38.5 | | 0.003 | 0.06 | N/U | | |
| | | 33.0 | | 0.013 | 0.62 | N/U | | |
| | | 24.2 | | 1.58 | T | N/ERA | | |
| SR80 | 40 | 44.0 | 86.6 | 0.002 | 0.007 | N/U | 30 33 78 104 171 1003 7082 | 22.3 21.3 15.7 16.6 13.9 11.7 10.0 |
| | | 38.5 | | 0.003 | 0.06 | N/U | | |
| | | 33.0 | | 0.013 | 0.62 | N/U | | |
| | | 24.2 | | 1.58 | T | N/ERA | | |

Table 3 - Stress-rupture Data for Tensar Geogrids (Sheet 2 of 2)

| Type | Temperature °C | Load kN/m | Mean batch strength kN/m | Time to 10% strain h | Time to failure h | Source and verification | Last measured strain | |
|-------|----------------|-----------|--------------------------|----------------------|-------------------|-------------------------|----------------------|----------|
| | | | | | | | Time h | Strain % |
| SR110 | 10 | 75.77 | 122.5 | 0.79 | 42.5 | N/U | 27.5 | 18.7 |
| | | 73.92 | | 1.1 | 63 | N/U | 45.4 | 18.6 |
| | | 69.96 | | 2.0 | 405 | N/U | 336 | 28.1 |
| | | 63.35 | | 7.8 | 864 | N/U | 864 | 20.7 |
| | | 58.67 | | 64.6 | T | N/U | 310 | 11.3 |
| SR110 | 20 | 65.5 | 122.5 | 0.56 | 35 | N/U | 30 | 23.0 |
| | | 64.9 | | 0.81 | 42 | N/U | 33 | 22.7 |
| | | 55 | | 25.1 | 1598 | N/BBA | 1539 | 16.8 |
| | | 51.5 | | 166 | 4151 | N/BBA | 4128 | 13.4 |
| | | 45.3 | | 25118 | T | N/BBA | 30888 | 10.1 |
| SR110 | 40 | 51.5 | 122.5 | 0.78 | T | N/ERA | 7 | 12.1 |
| | | 45.3 | | 30.5 | 1849 | N/ERA | 1758 | 13.3 |
| SR2 | 20-23 | 47 | 84.6 | 0.23 | 28 | ERA | 26 | 23.7 |
| | | 39 | | 5 | 496 | ERA | 496* | 19 |
| | | 35 | | 77 | 8444 | ERA | 8405 | 15.4 |
| | | 31.3 | | 7200 | 11374 | ERA | 11350 | 11.0 |
| | | 31.3 | | 7100 | T | N/U | 15915 | 10.5 |
| | | 31.3 | | >16757 | C | ERA | 16757 | 9.6 |
| SR2 | 40 | 35.8 | 85.4 | 0.3 | 10 | N/ERA | 10 | 14.4 |
| | | 32.0 | | 7 | T | N/ERA | 66 | 11.8 |
| | | 28.7 | | 280 | T | N/ERA | 380 | 10.3 |
| | | 24.0 | | >10000 | T | N/ERA | 10000 | 8.3 |

Key :

Time to failure

T terminated without rupture

C test continues

* to within 24 h

Source and verification

N/BBA Netlon data submitted to and accepted by British Board of Agrément

N/ERA Netlon data submitted to GCO and verified by ERA

N/U unverified Netlon internal data

ERA independent ERA Test

LIST OF FIGURES

| Figure No. | | Page No. |
|------------|--|----------|
| 1 | Strain versus Time to Failure for Varying Stress Levels (Schematic) | 40 |
| 2 | Typical Stress-rupture Curve for Unoriented Polyethylene | 41 |
| 3 | Extrapolation of Stress-rupture Data for 50 Year Lifetime Prediction | 42 |
| 4 | Use of Elevated Temperature Data to Extrapolate Ambient Data (Schematic) | 43 |
| 5 | Crystal Structure in Polyethylene (Schematic) | 44 |
| 6 | The Ductile Deformation Process of Unoriented Polyethylene (Schematic) | 45 |
| 7 | Brittle Failure of Unoriented Polyethylene (Schematic) | 46 |
| 8 | Long Branches Excluded from Lamellar Lattice (Schematic) | 47 |
| 9 | Short Chain Branches Act as Profusions and Inhibit Slip of Molecules (Schematic) | 48 |
| 10 | Input Data for Tensar SR55 at 10°C | 49 |
| 11 | Input Data for Tensar SR55 at 20°C | 50 |
| 12 | Input Data for Tensar SR55 at 40°C | 51 |
| 13 | Input Data for Tensar SR80 at 10°C | 52 |
| 14 | Input Data for Tensar SR80 at 20°C | 53 |
| 15 | Input Data for Tensar SR80 at 40°C | 54 |
| 16 | Input Data for Tensar SR110 at 10°C | 55 |
| 17 | Input Data for Tensar SR110 at 20°C | 56 |
| 18 | Input Data for Tensar SR110 at 40°C | 57 |
| 19 | Input Data for Tensar SR2 at 20°C | 58 |
| 20 | Input Data for Tensar SR2 at 40°C | 59 |

| Figure No. | | Page No. |
|---------------|---|-------------|
| 21 | Normalised Data for Tensars SR55, SR80 and SR110 at 10°C | 60 |
| 22 | Normalised Data for Tensars SR55, SR80 and SR110 at 20°C | 61 |
| 23 | Normalised Data for Tensars SR55, SR80 and SR110 at 40°C | 62 |
| 24 | Times to 10% Strain for Tensars SR55, SR80 and SR110 Shifted to 35°C with 95% Confidence Limit | 63 |
| 25 | Times to Rupture Shifted to 35°C for Tensars SR55, SR80 and SR110 with 95% Confidence Limit | 64 |
| 26 | Times to 10% Strain for Tensar SR2 Shifted to 35°C with 95% Confidence Limit | 65 |
| 27 | Times to Rupture Shifted to 35°C for Tensar SR2 with 95% Confidence Limit | 66 |
| 28 | Relative Load Plotted against Log (Log (Hours to Failure)) for Tensar SR2 Showing Hyperbolic Nature of Confidence Limit | 67 |
| 29 | Calculation of Design Required Force (See Ref. 39) | 68 |

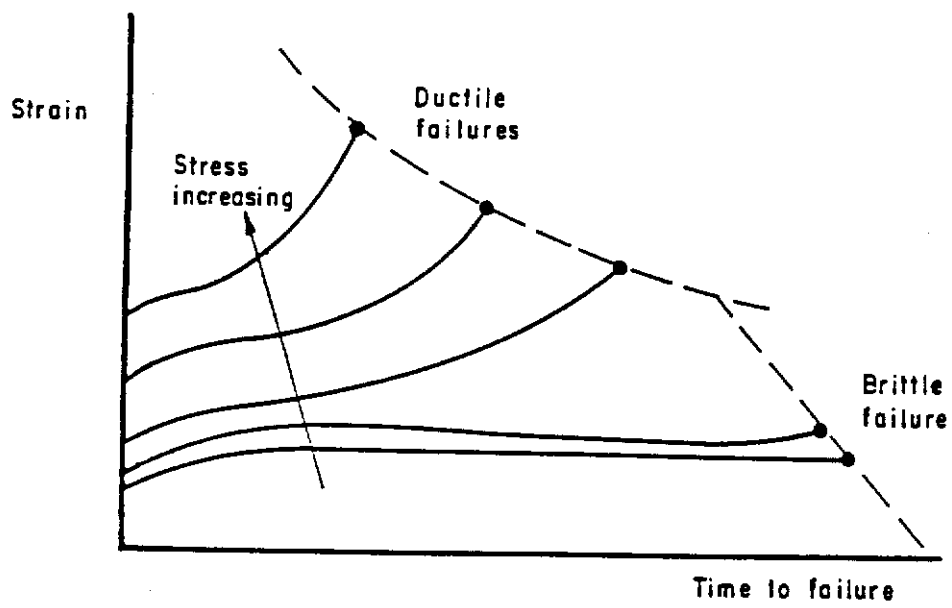


Figure 1 - Strain versus Time to Failure for Varying Stress Levels (Schematic)

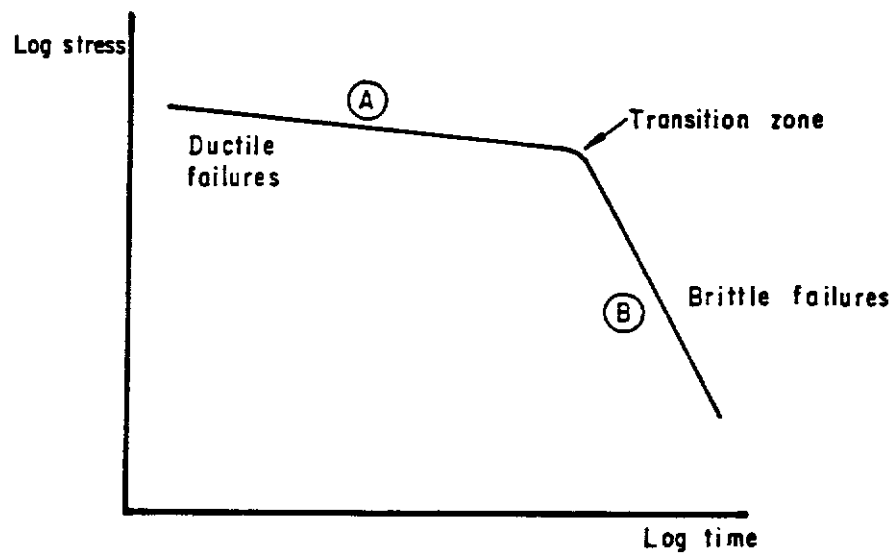


Figure 2 - Typical Stress-rupture Curve for Unoriented Polyethylene

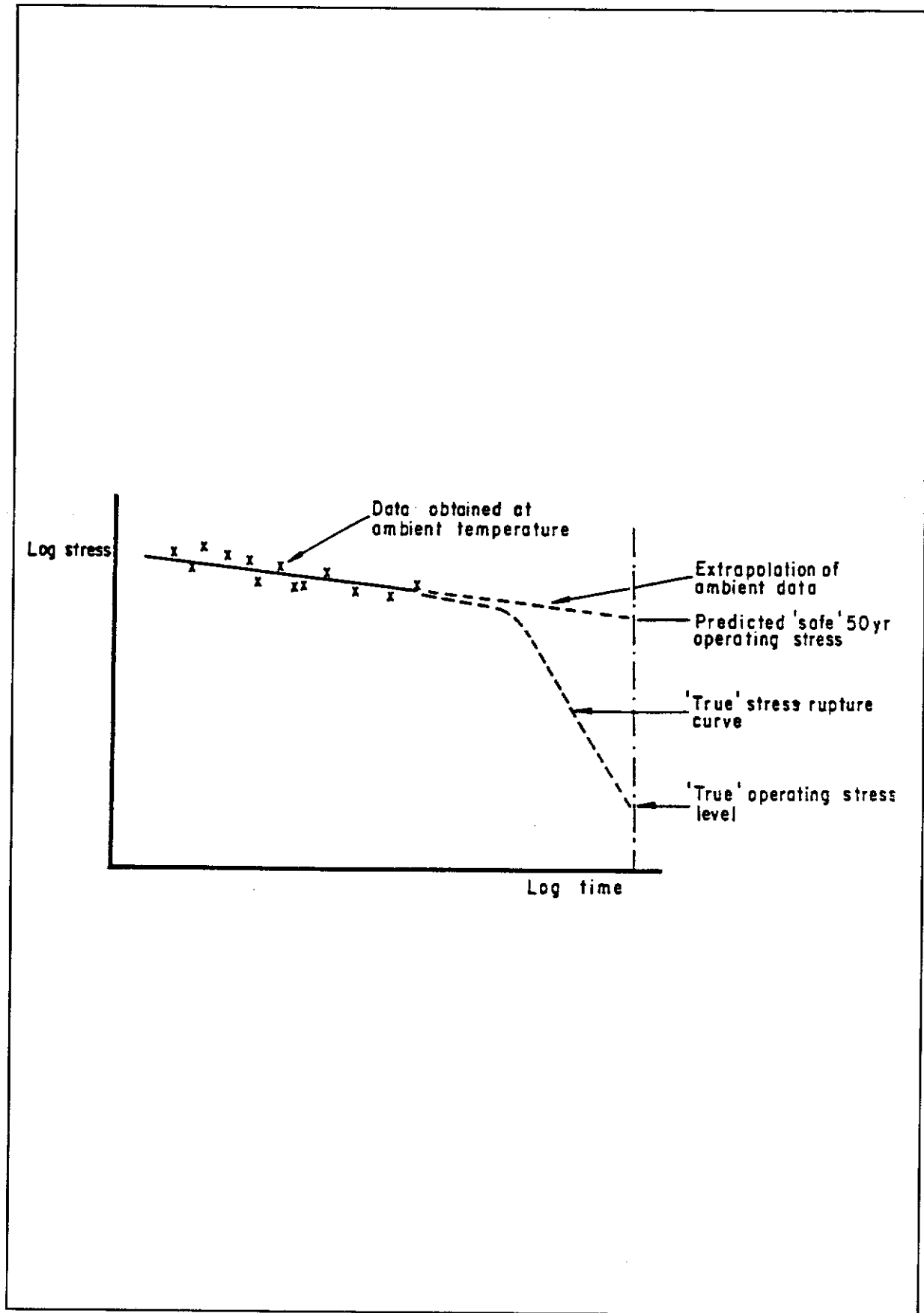


Figure 3 - Extrapolation of Stress-rupture Data for 50 Year Lifetime Prediction

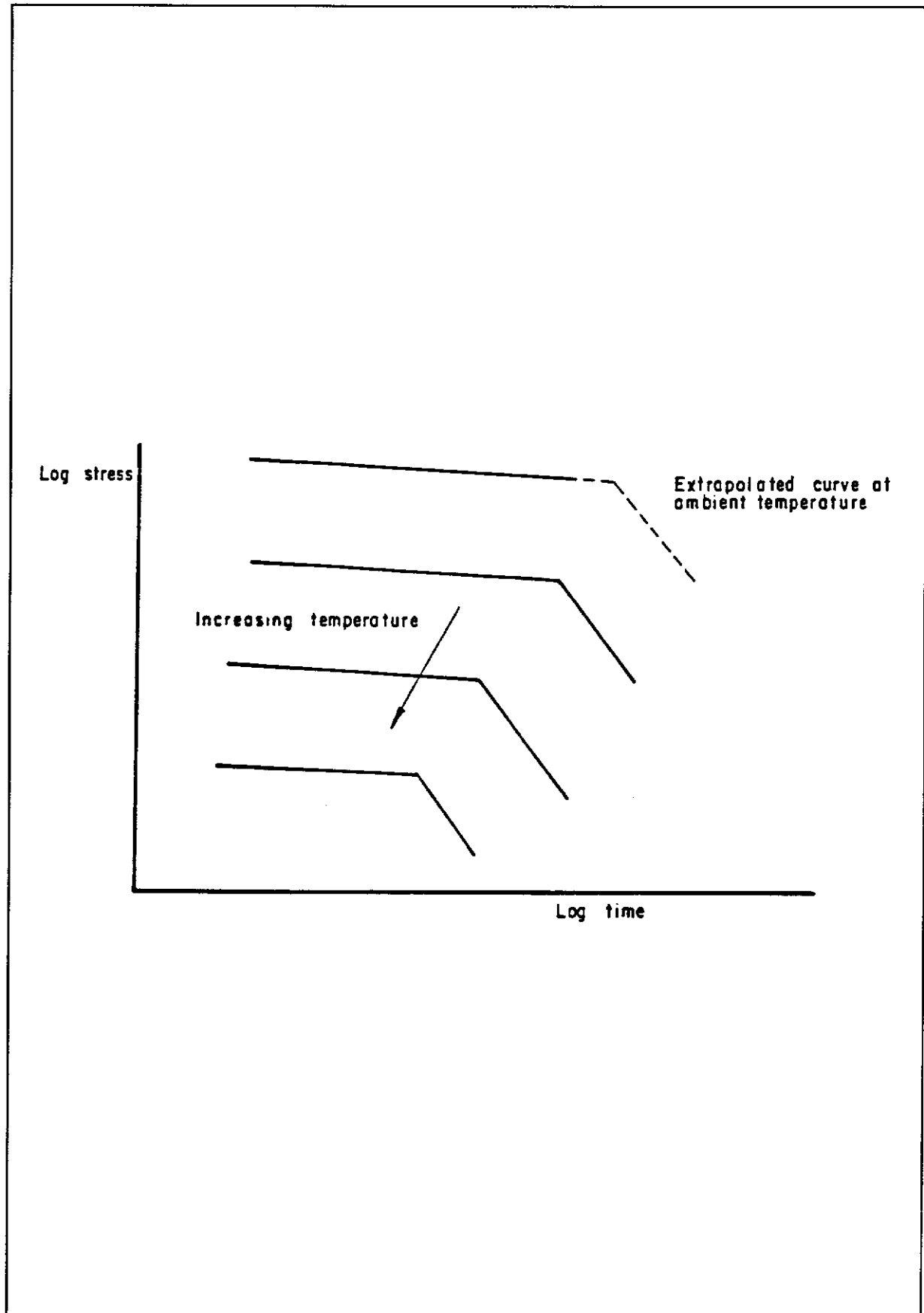


Figure 4 - Use of Elevated Temperature Data to Extrapolate Ambient Data (Schematic)

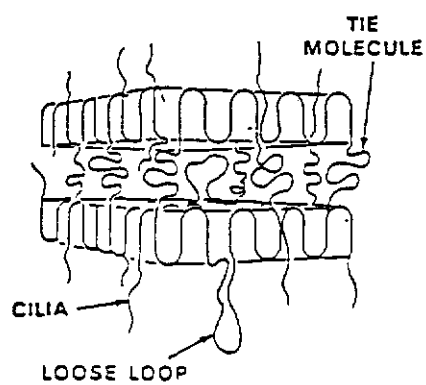


Figure 5 - Crystal Structure in Polyethylene (Schematic)

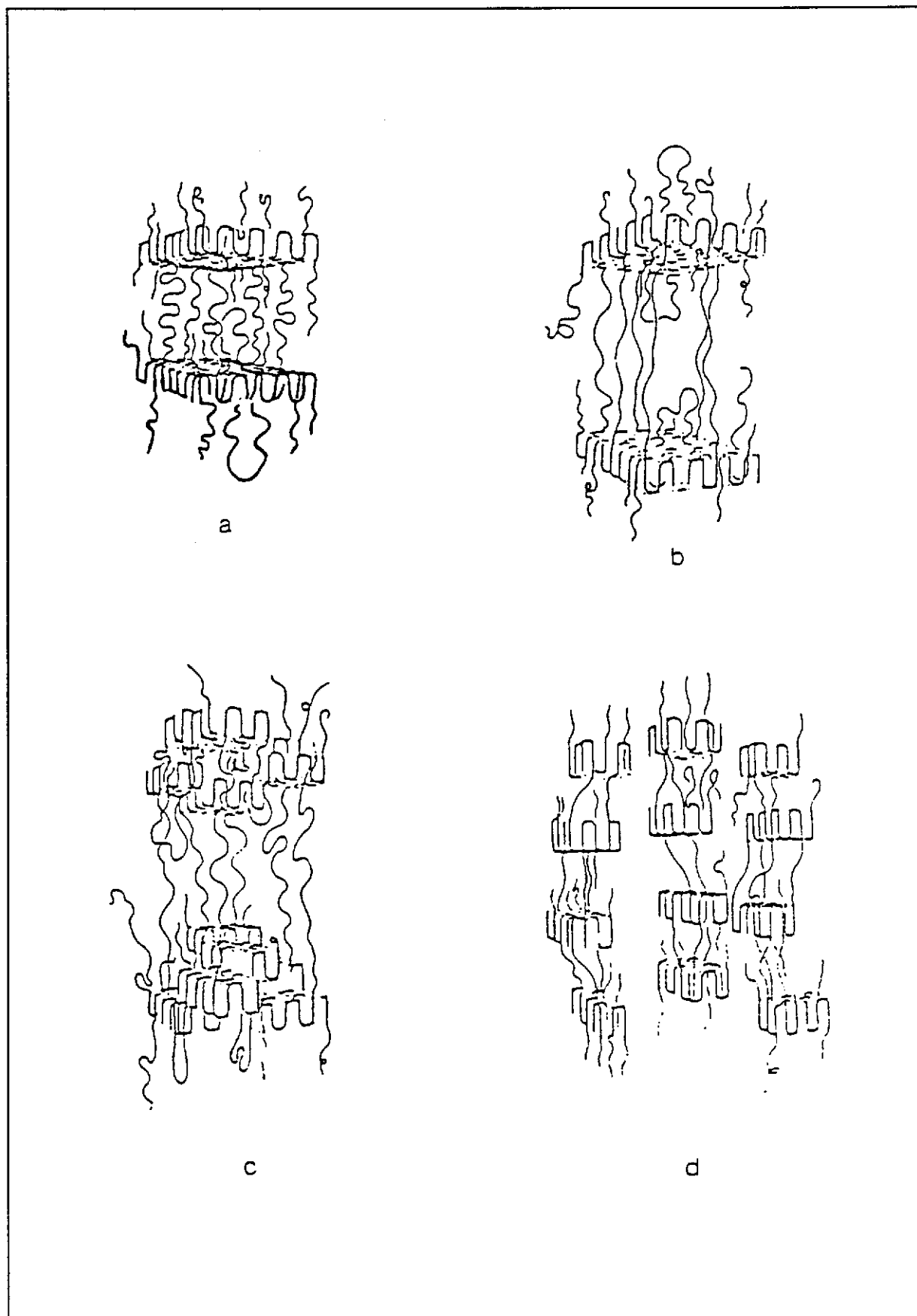


Figure 6 - The Ductile Deformation Process of Unoriented Polyethylene (Schematic)

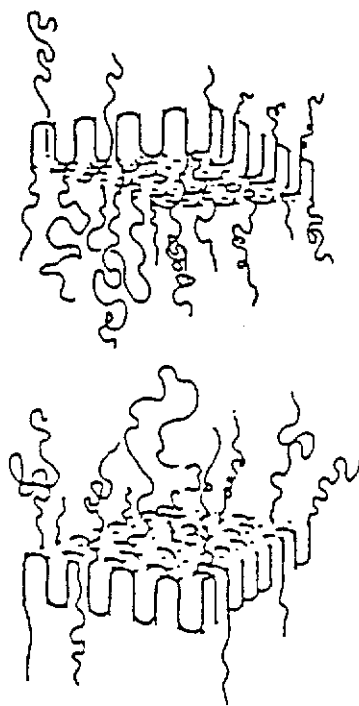


Figure 7 - Brittle Failure of Unoriented Polyethylene (Schematic)

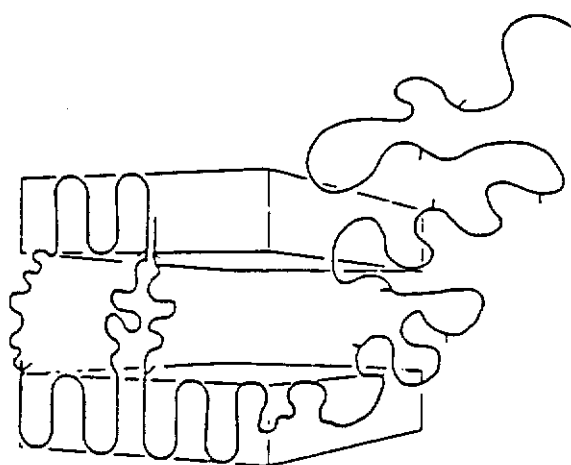


Figure 8 - Long Branches Excluded from Lamellar Lattice (Schematic)



Figure 9 - Short Chain Branches Act as Profusions and Inhibit Slip of Molecules (Schematic)

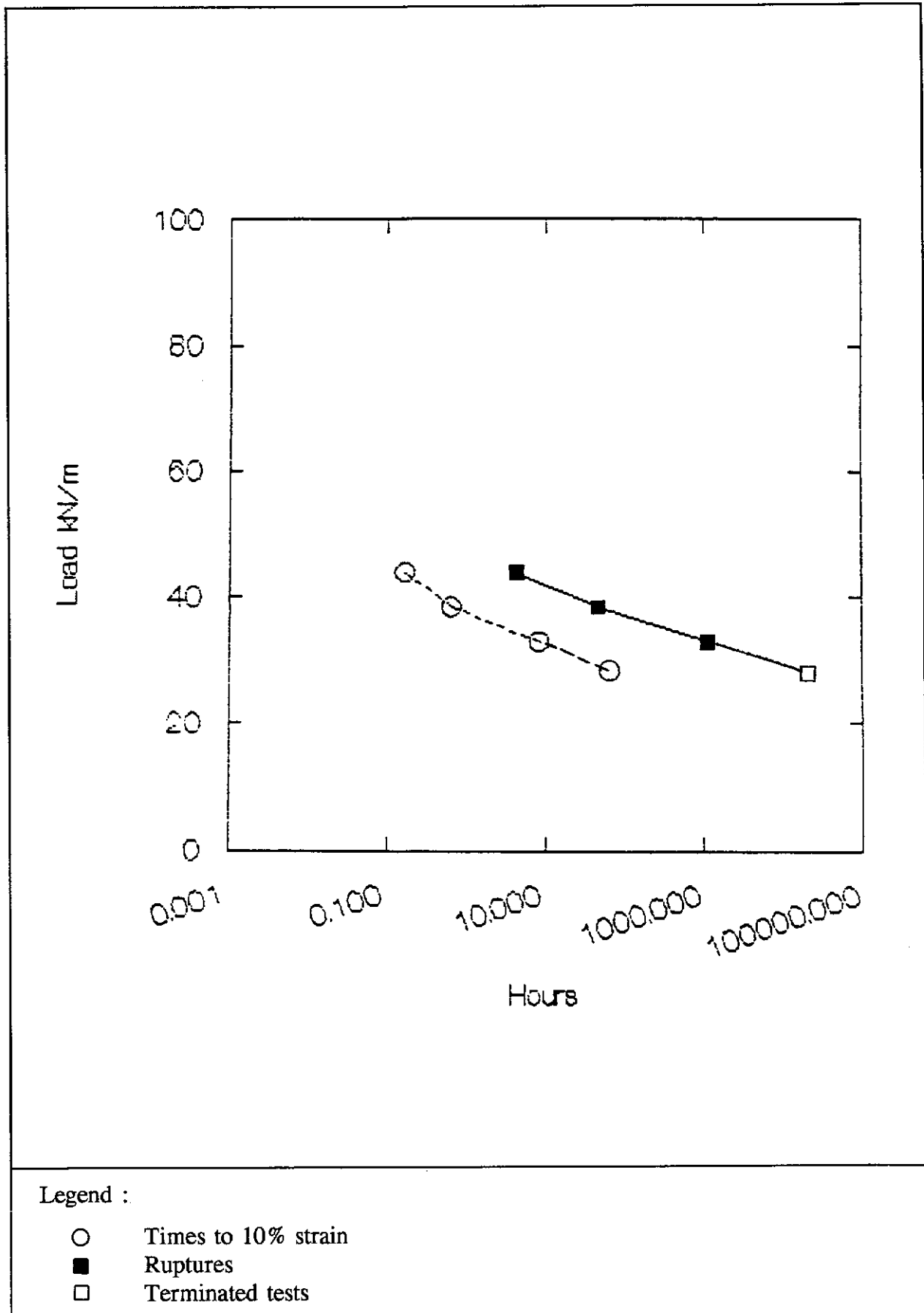


Figure 10 - Input Data for Tensar SR55 at 10°C

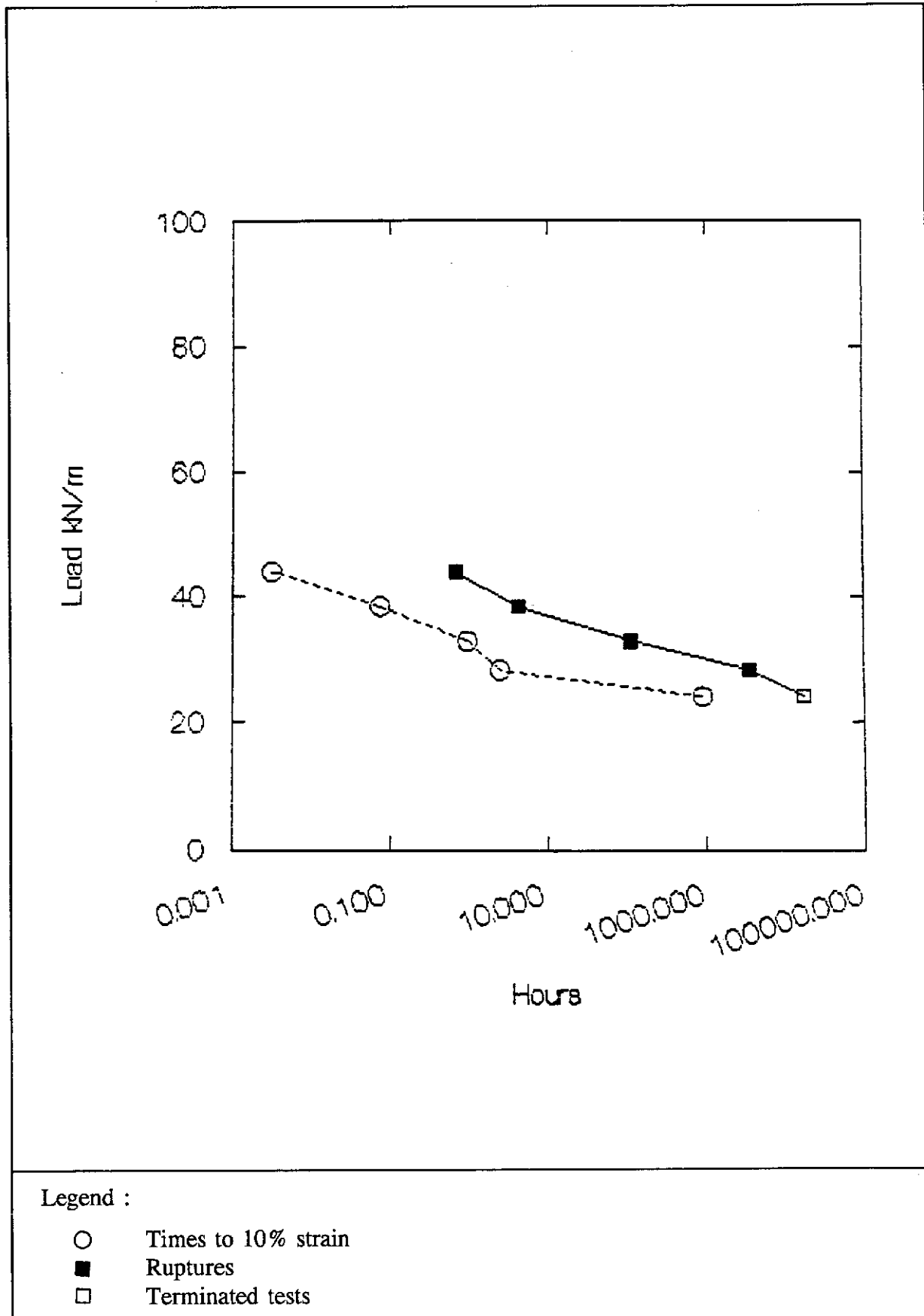


Figure 11 - Input Data for Tensar SR55 at 20°C

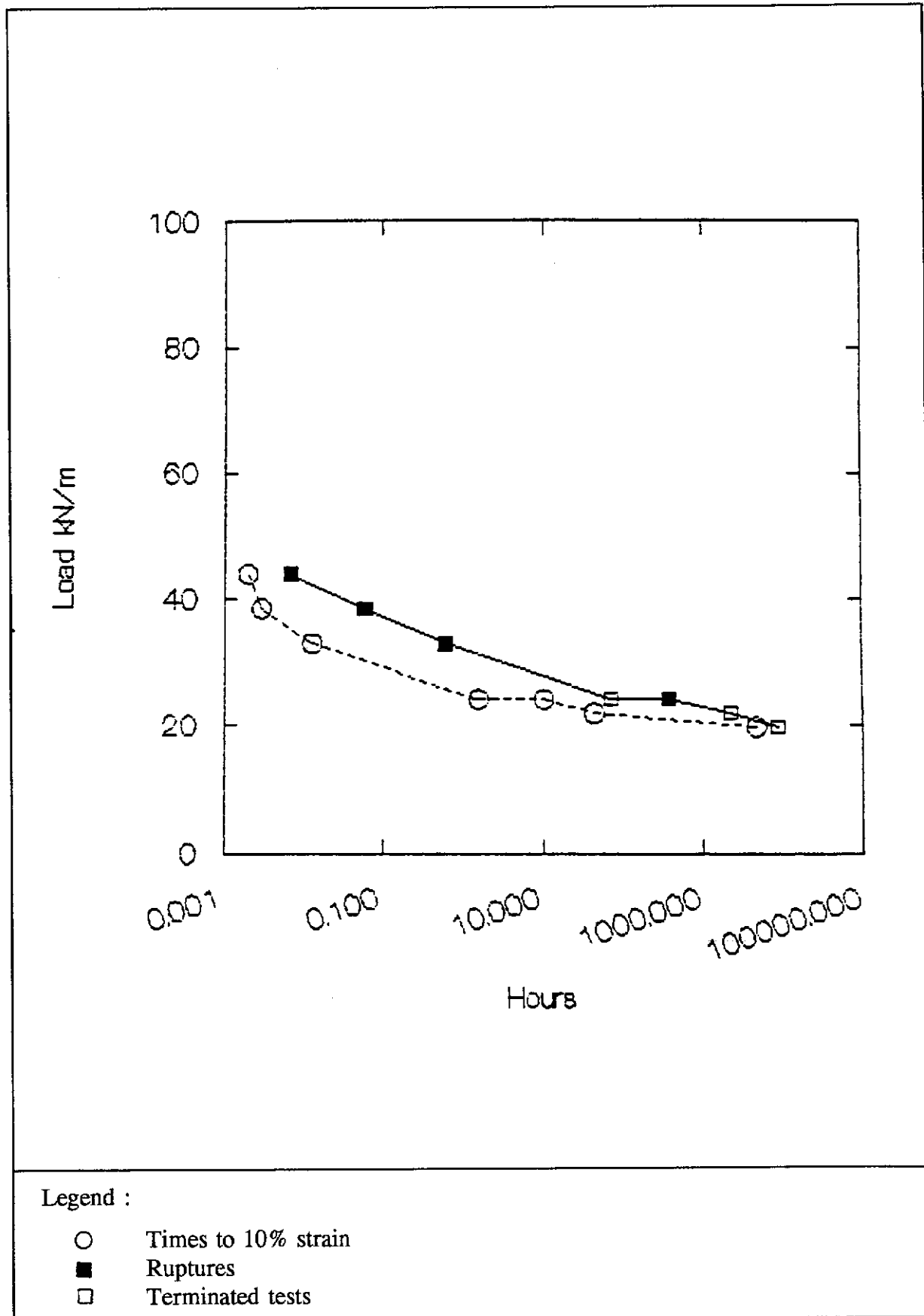
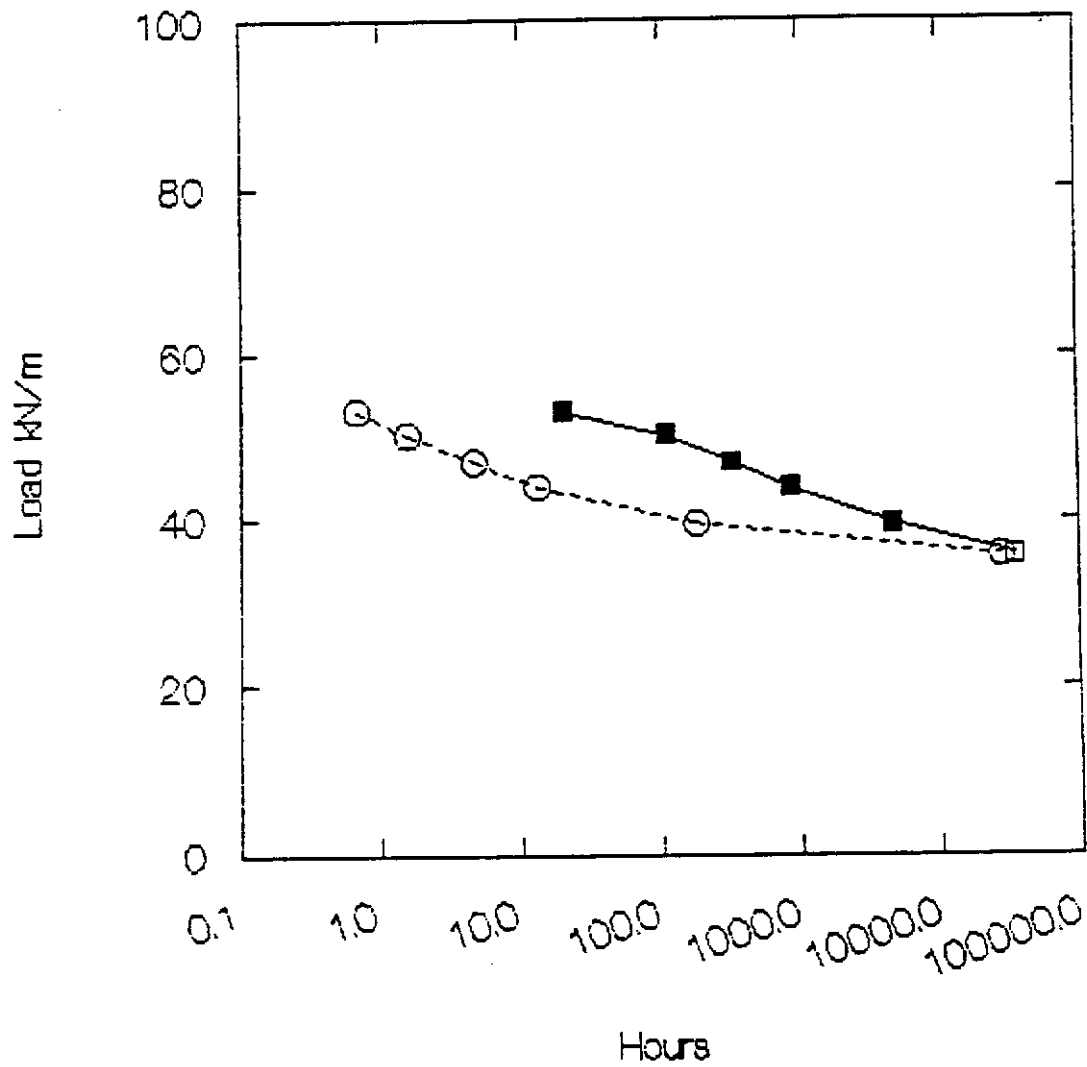


Figure 12 - Input Data for Tensar SR55 at 40°C



Legend :

- Times to 10% strain
- Ruptures
- Terminated tests

Figure 13 - Input Data for Tensar SR80 at 10°C

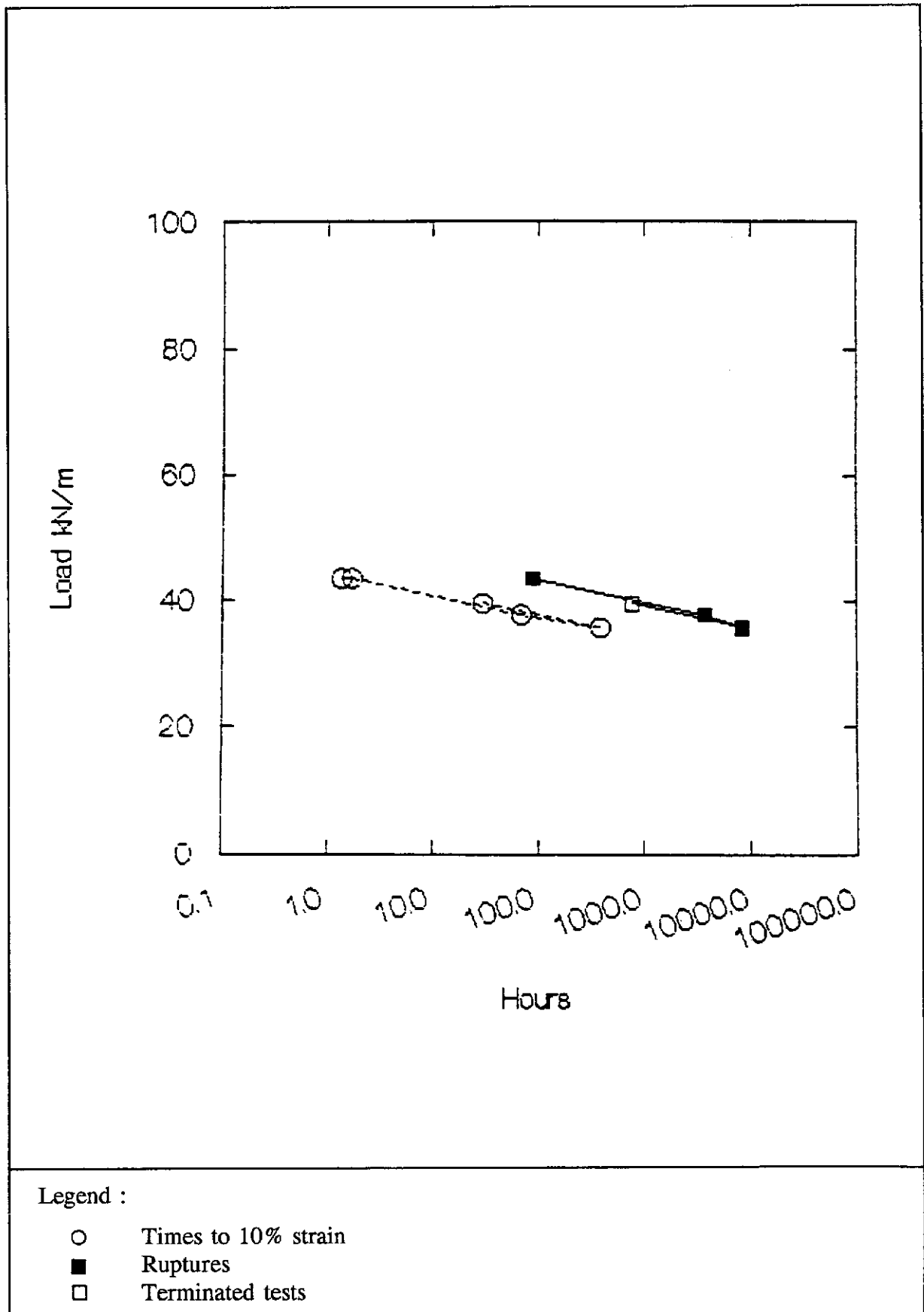


Figure 14 - Input Data for Tensar SR80 at 20°C

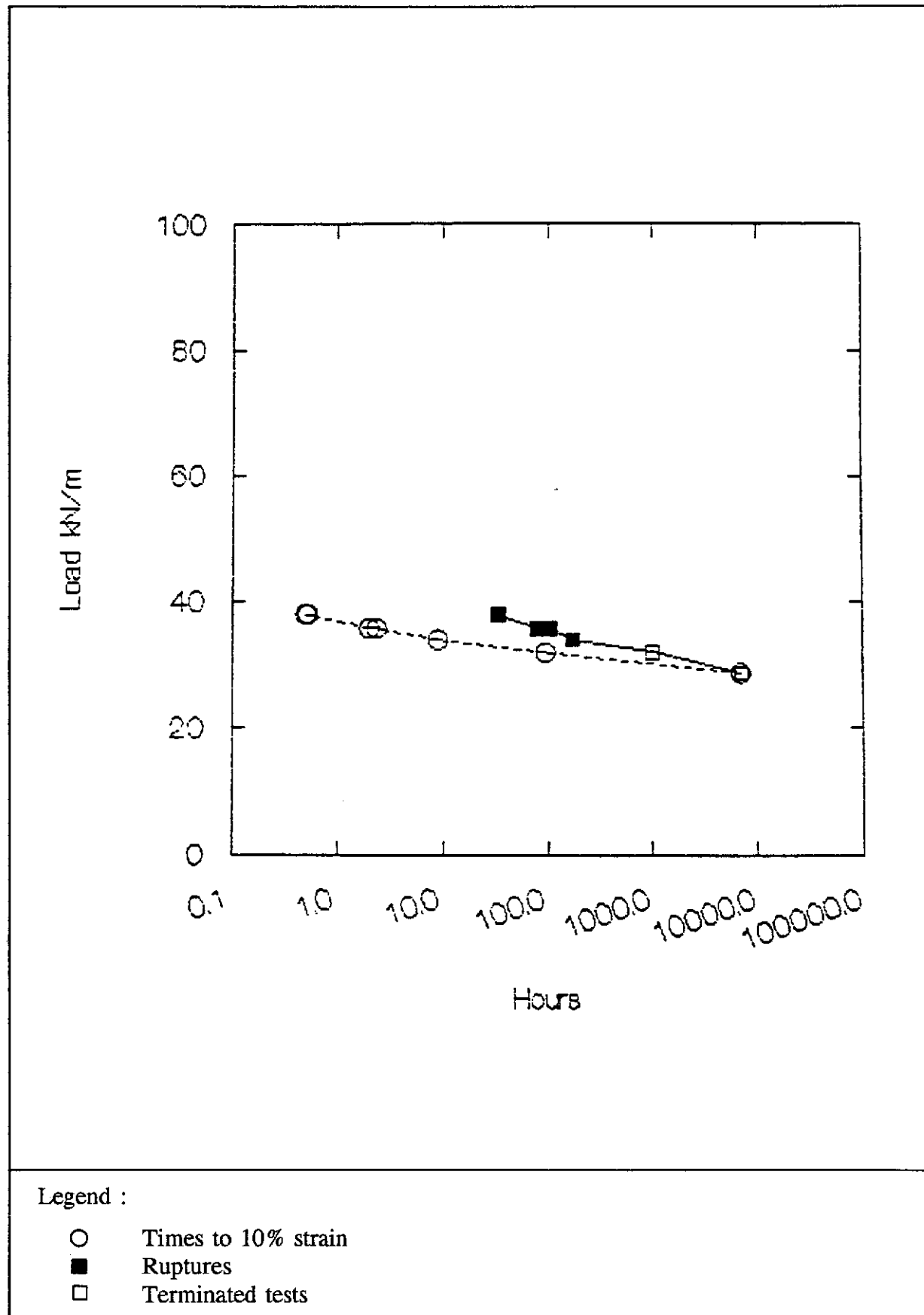
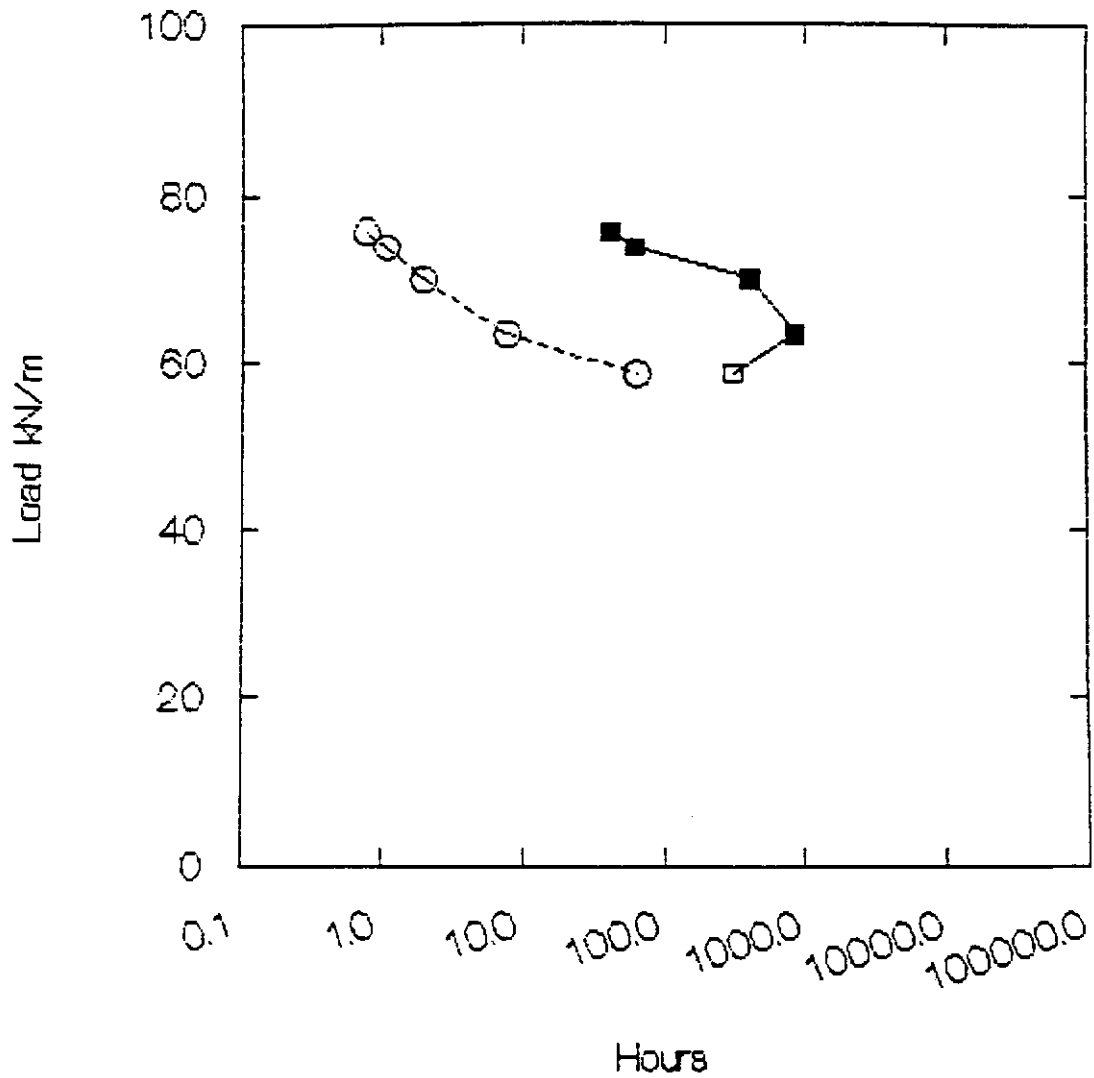


Figure 15 - Input Data for Tensar SR80 at 40°C



Legend :

- Times to 10% strain
- Ruptures
- Terminated tests

Figure 16 - Input Data for Tensar SR110 at 10°C

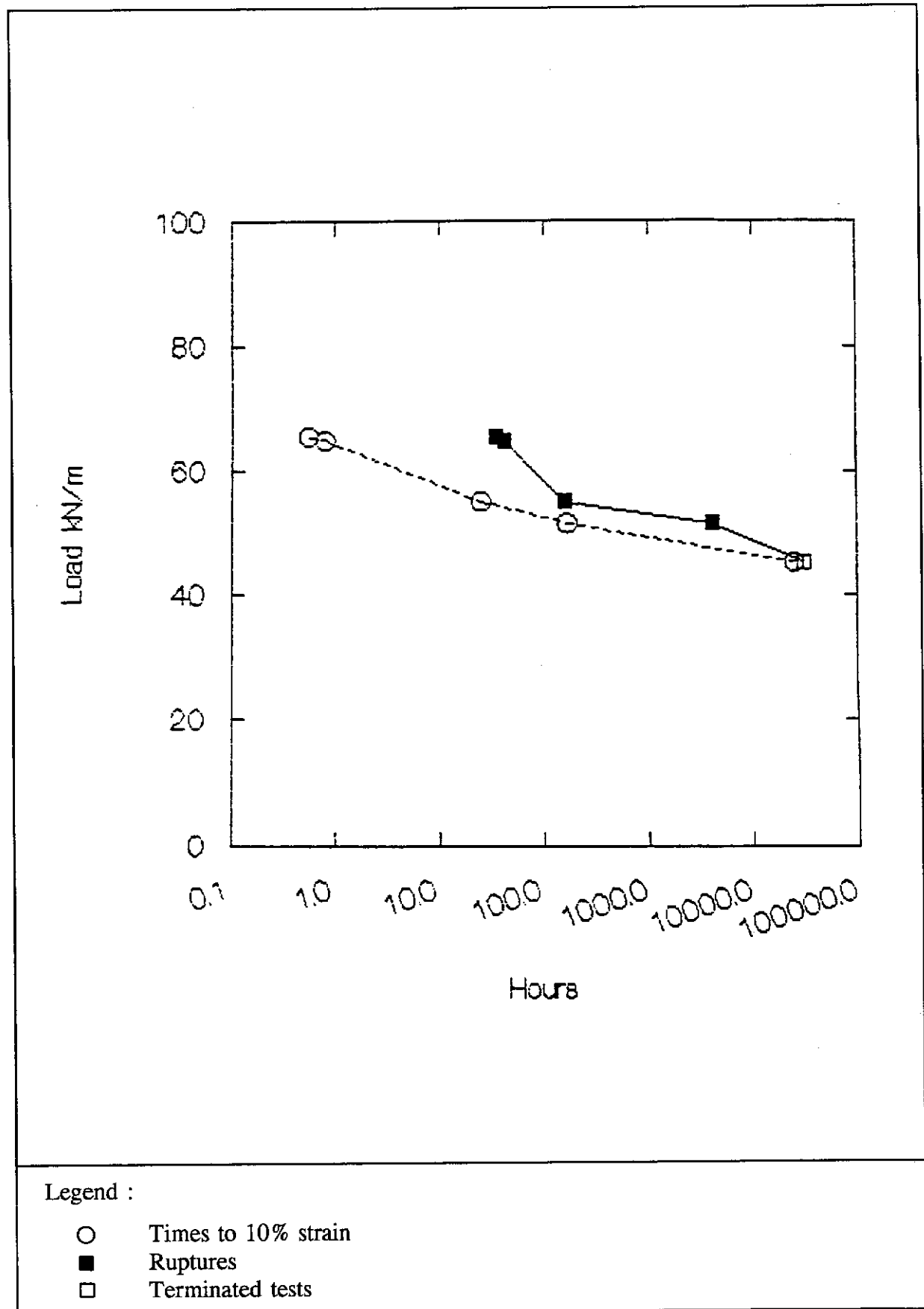


Figure 17 - Input Data for Tensar SR110 at 20°C

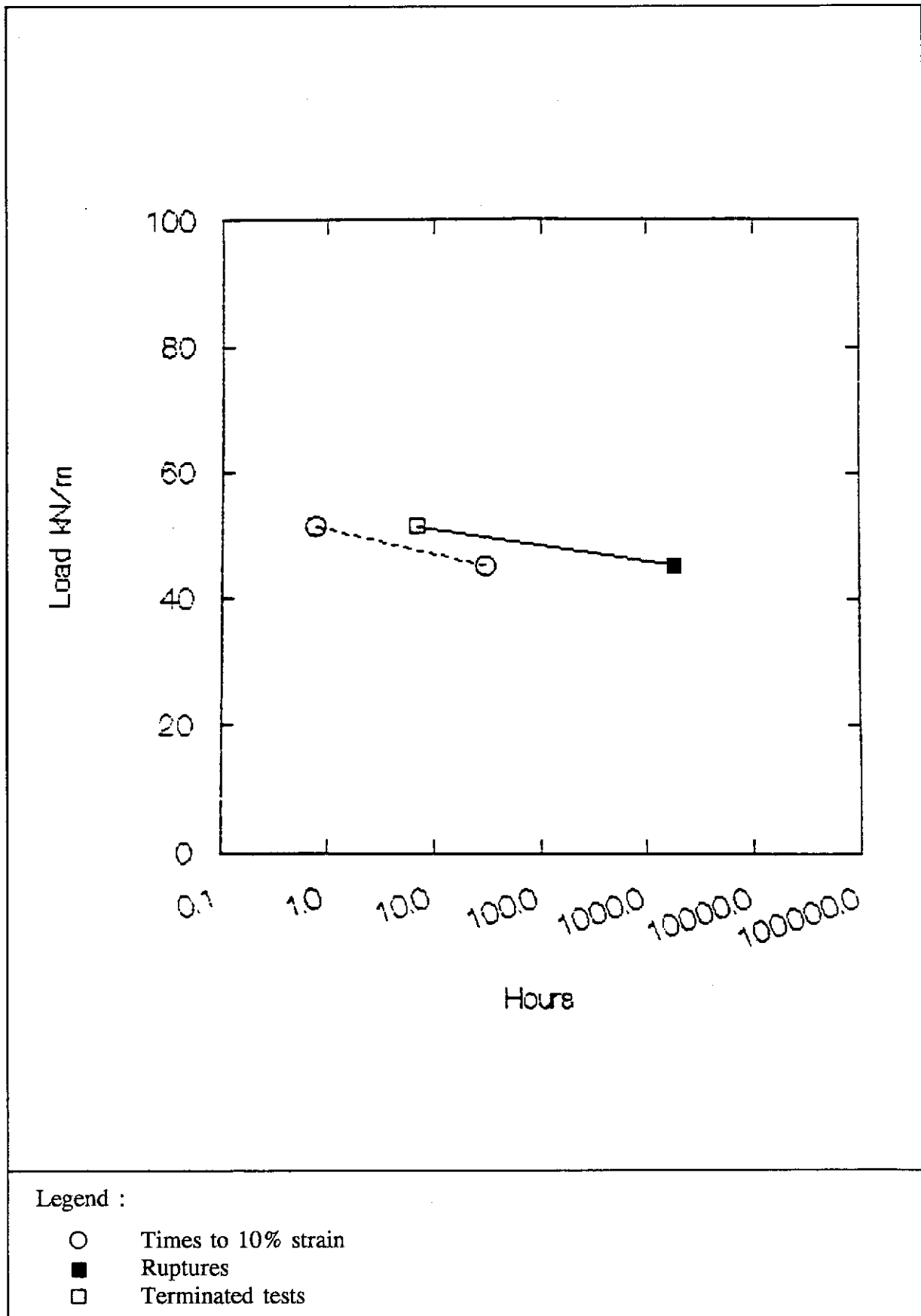


Figure 18 - Input Data for Tensar SR110 at 40°C

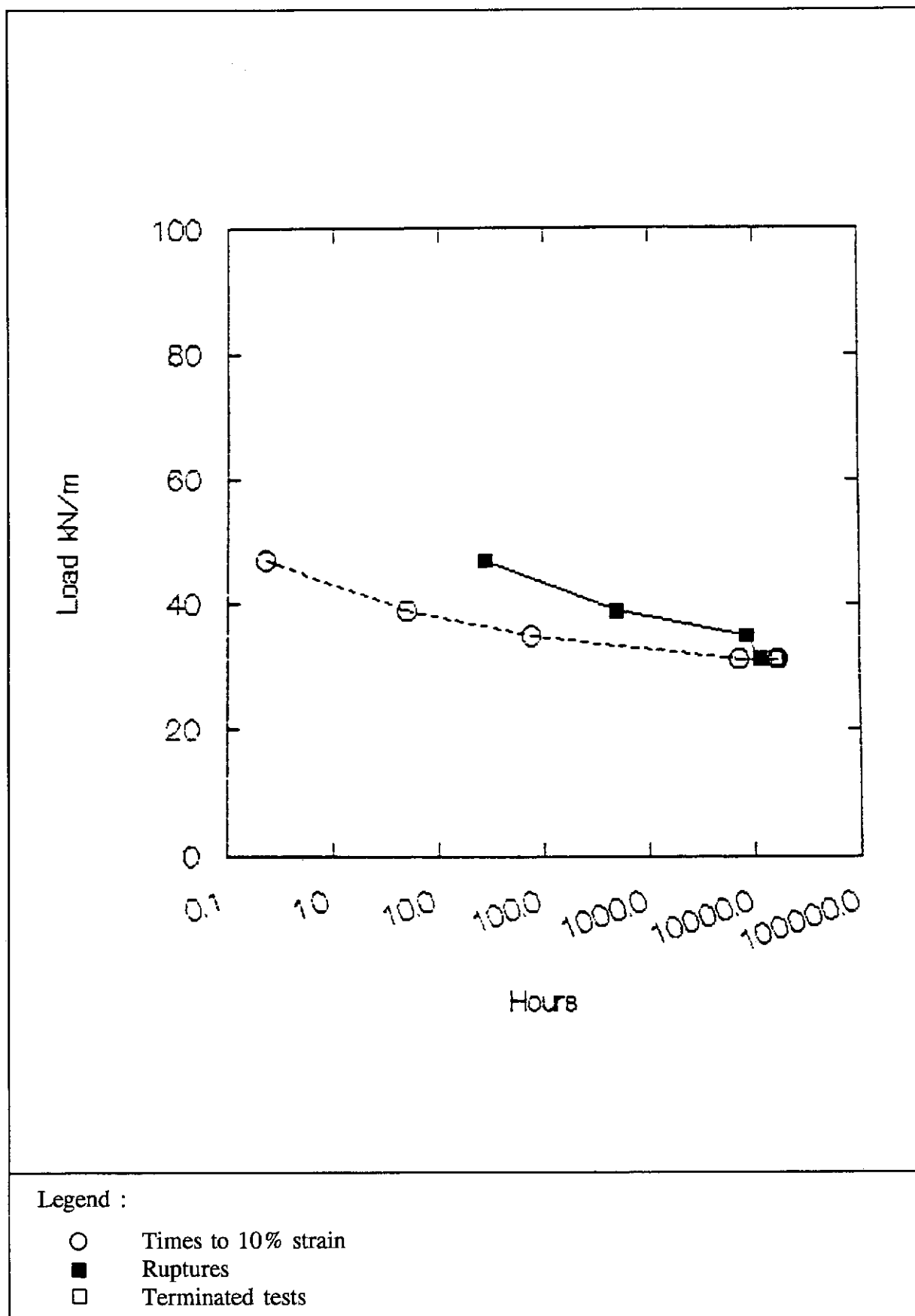


Figure 19 - Input Data for Tensar SR2 at 20°C

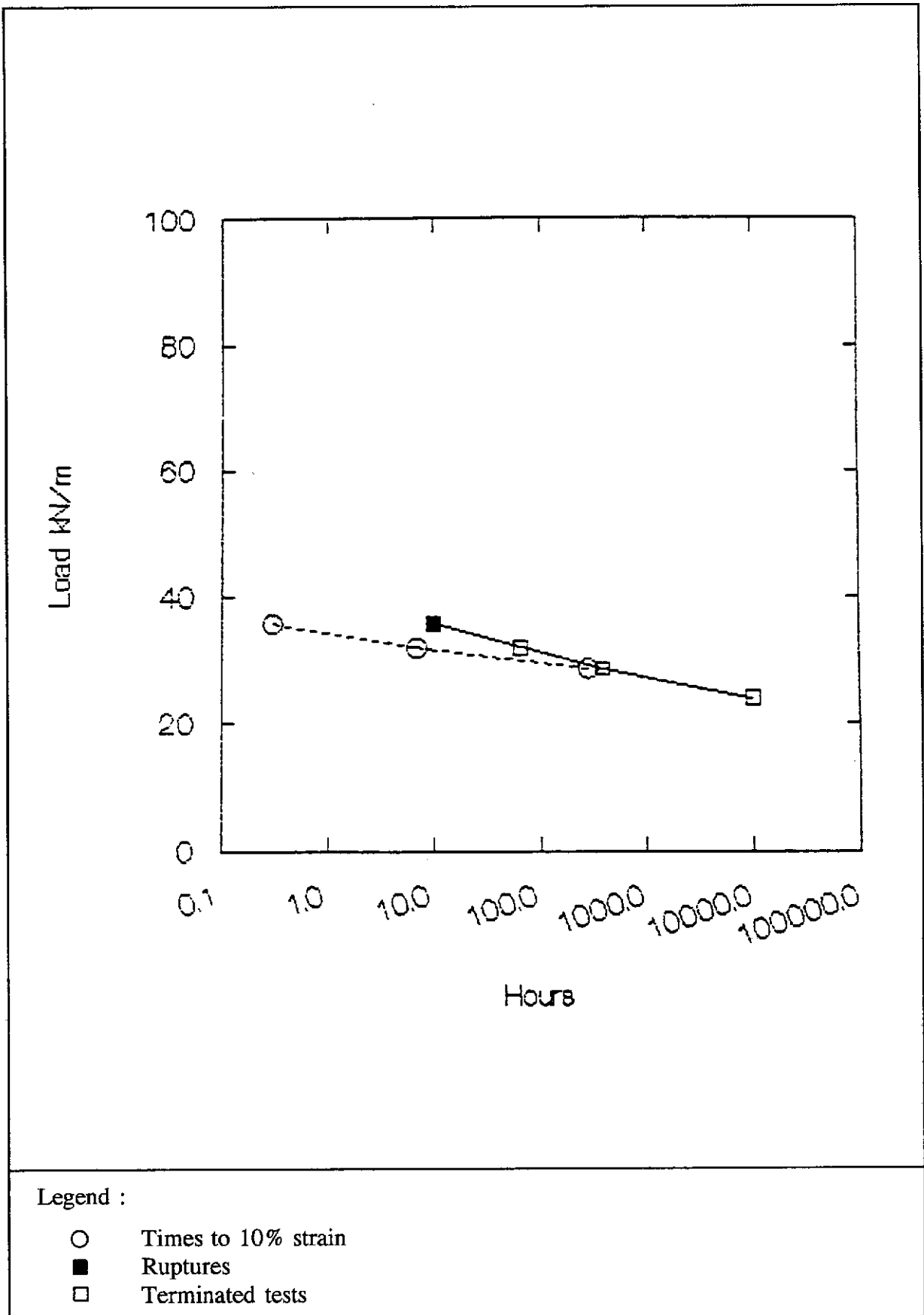


Figure 20 - Input Data for Tensar SR2 at 40°C

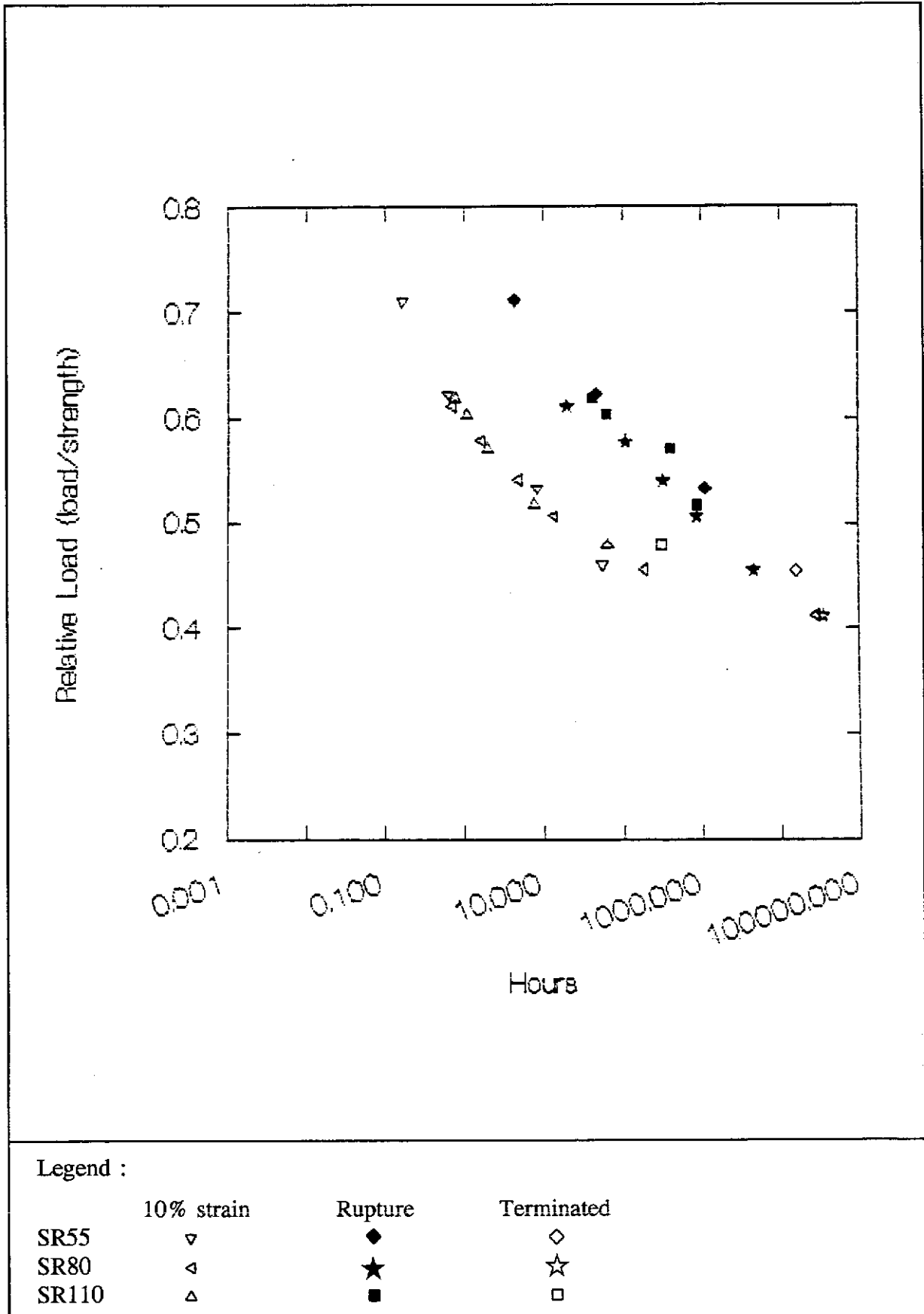


Figure 21 - Normalised Data for Tensars SR55, SR80 and SR110 at 10°C

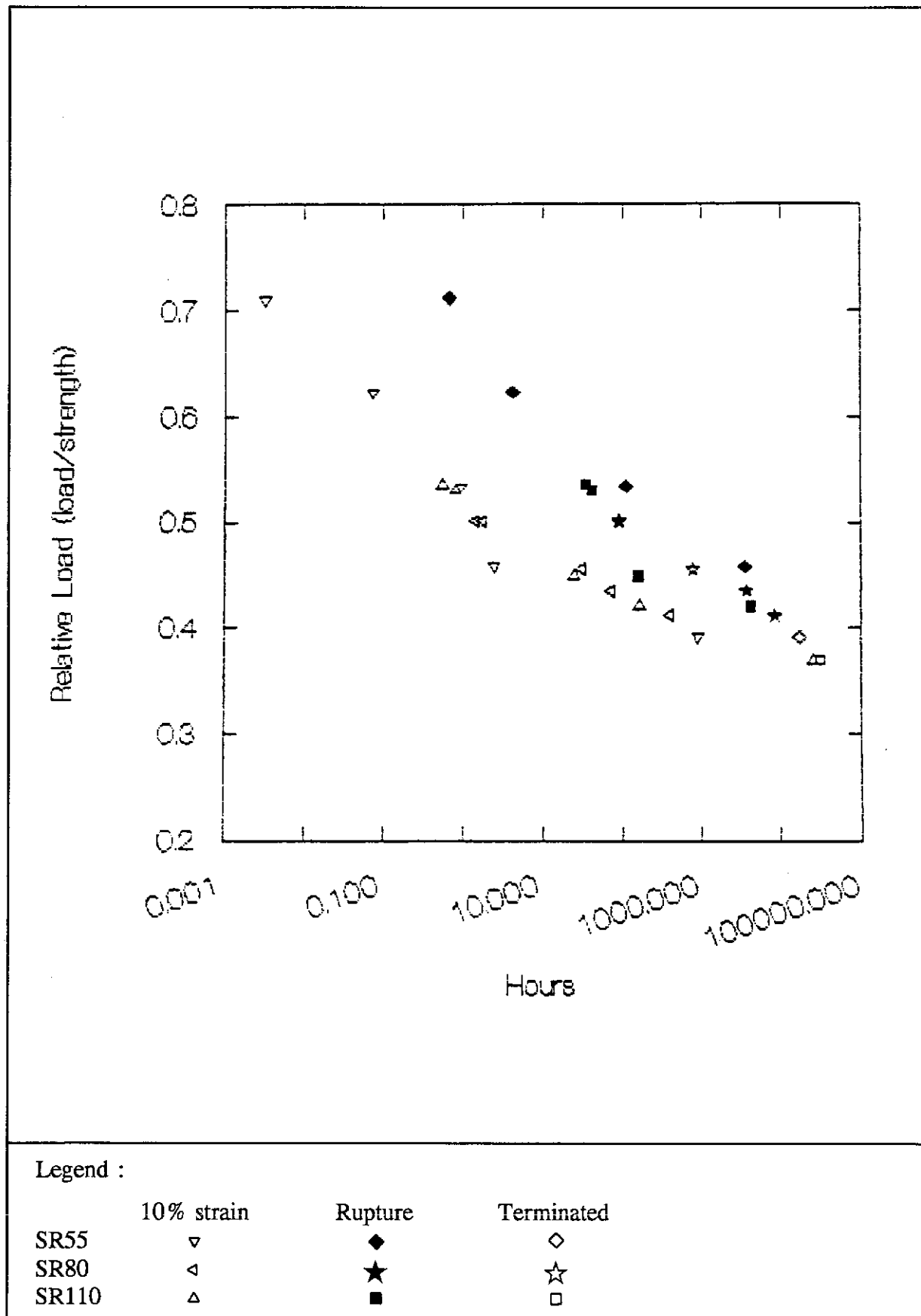


Figure 22 - Normalised Data for Tensars SR55, SR80 and SR110 at 20°C

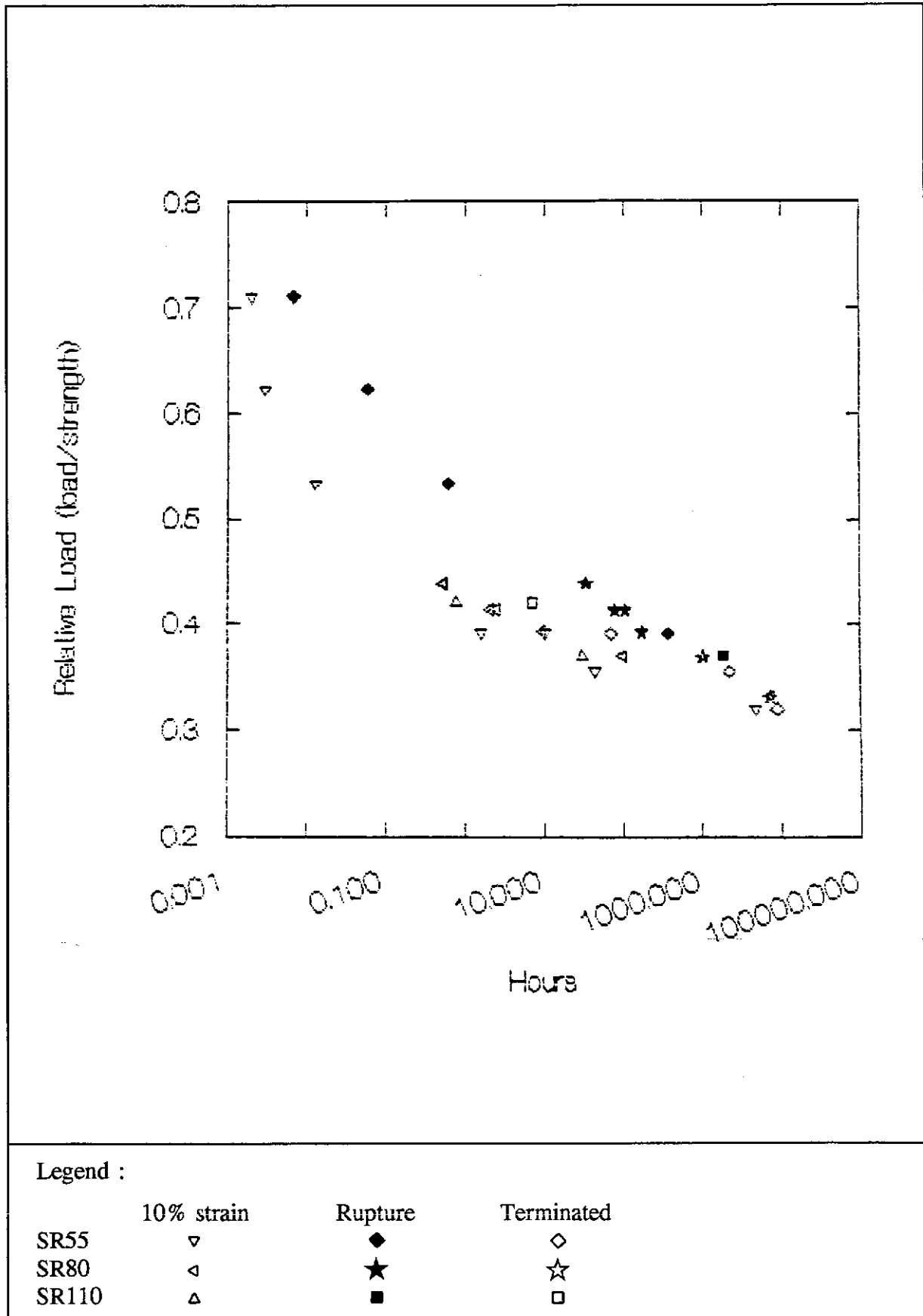
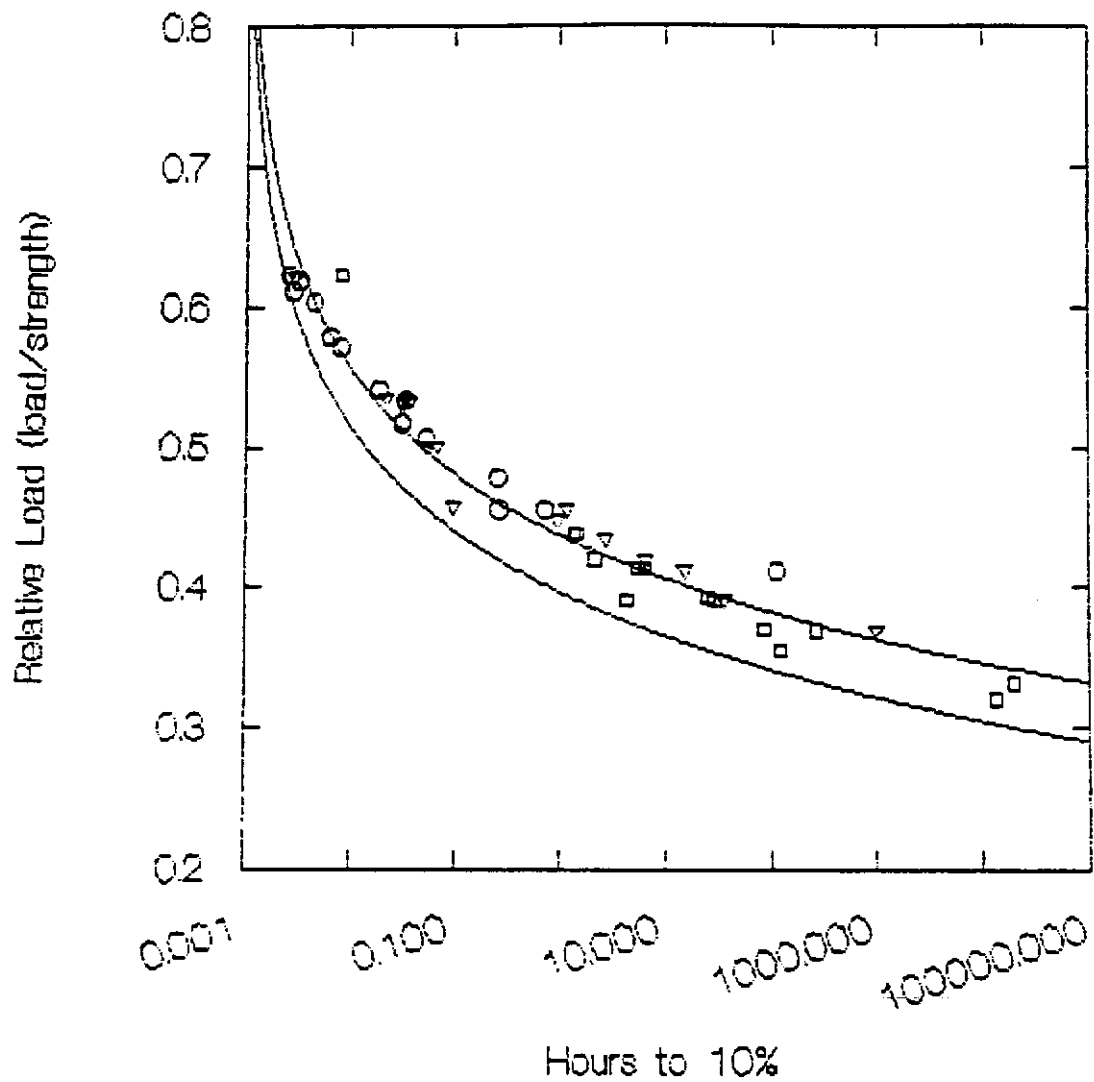


Figure 23 - Normalised Data for Tensars SR55, SR80 and SR110 at 40°C



Legend :

- 10°C
- ▽ 20°C
- 40°C

Figure 24 - Times to 10% Strain for Tensars SR55, SR80 and SR110 Shifted to 35°C with 95% Confidence Limit

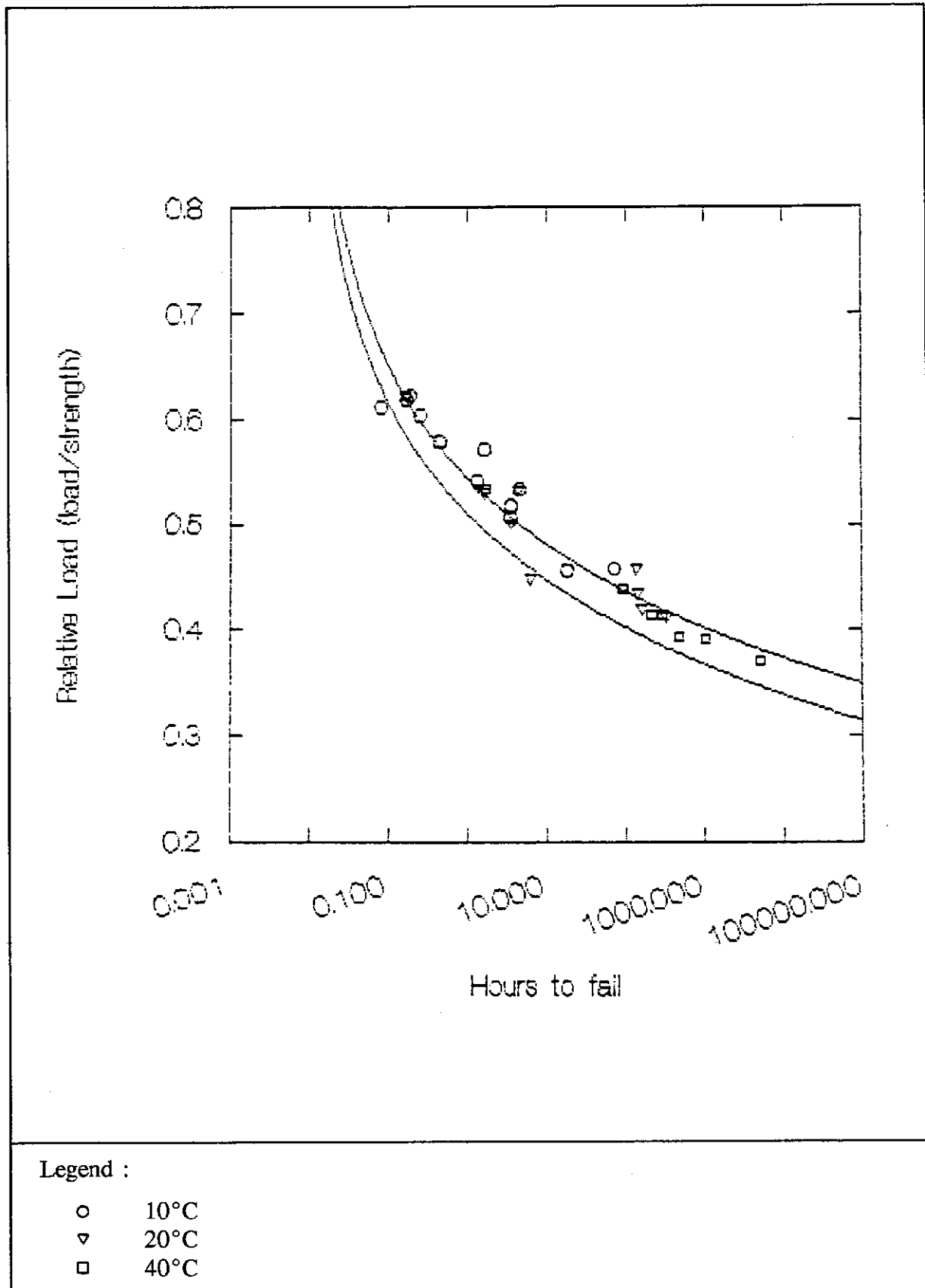


Figure 25 - Times to Rupture Shifted to 35°C for Tensars SR55, SR80 and SR110 with 95% Confidence Limit

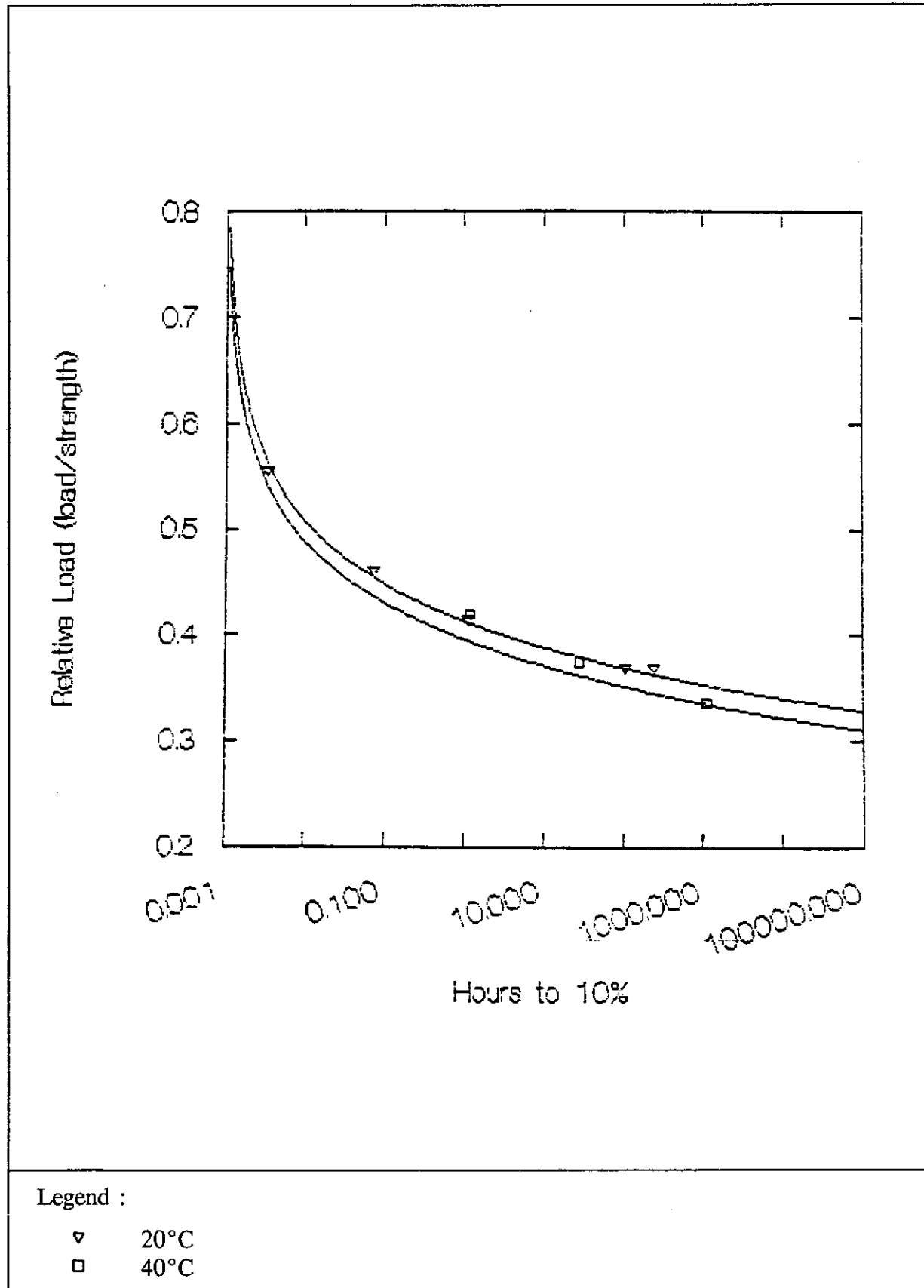


Figure 26 - Times to 10% Strain for Tensars SR2 Shifted to 35°C with 95% Confidence Limit

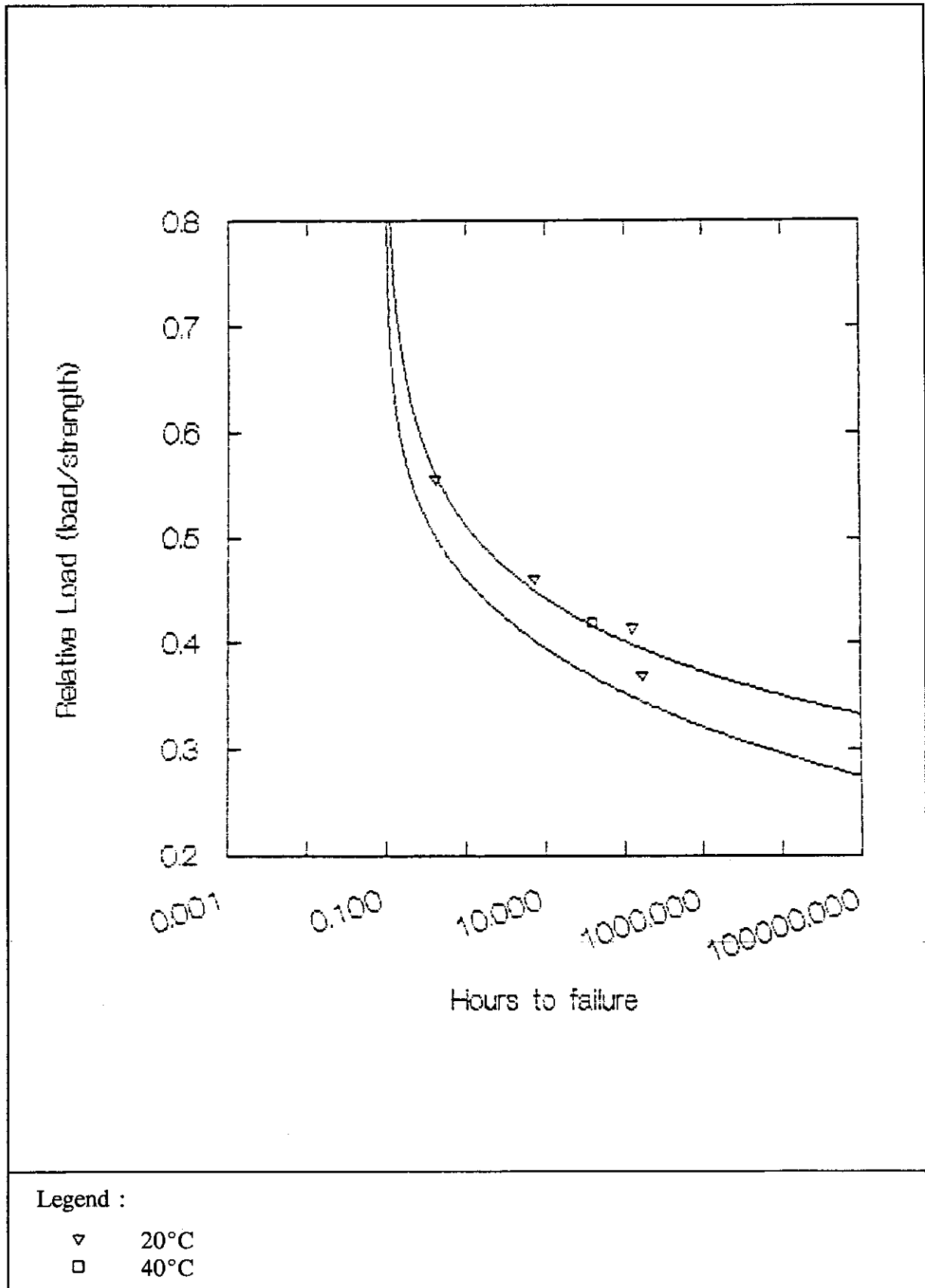


Figure 27 - Times to Rupture Shifted to 35°C for Tensar SR2
with 95% Confidence Limit

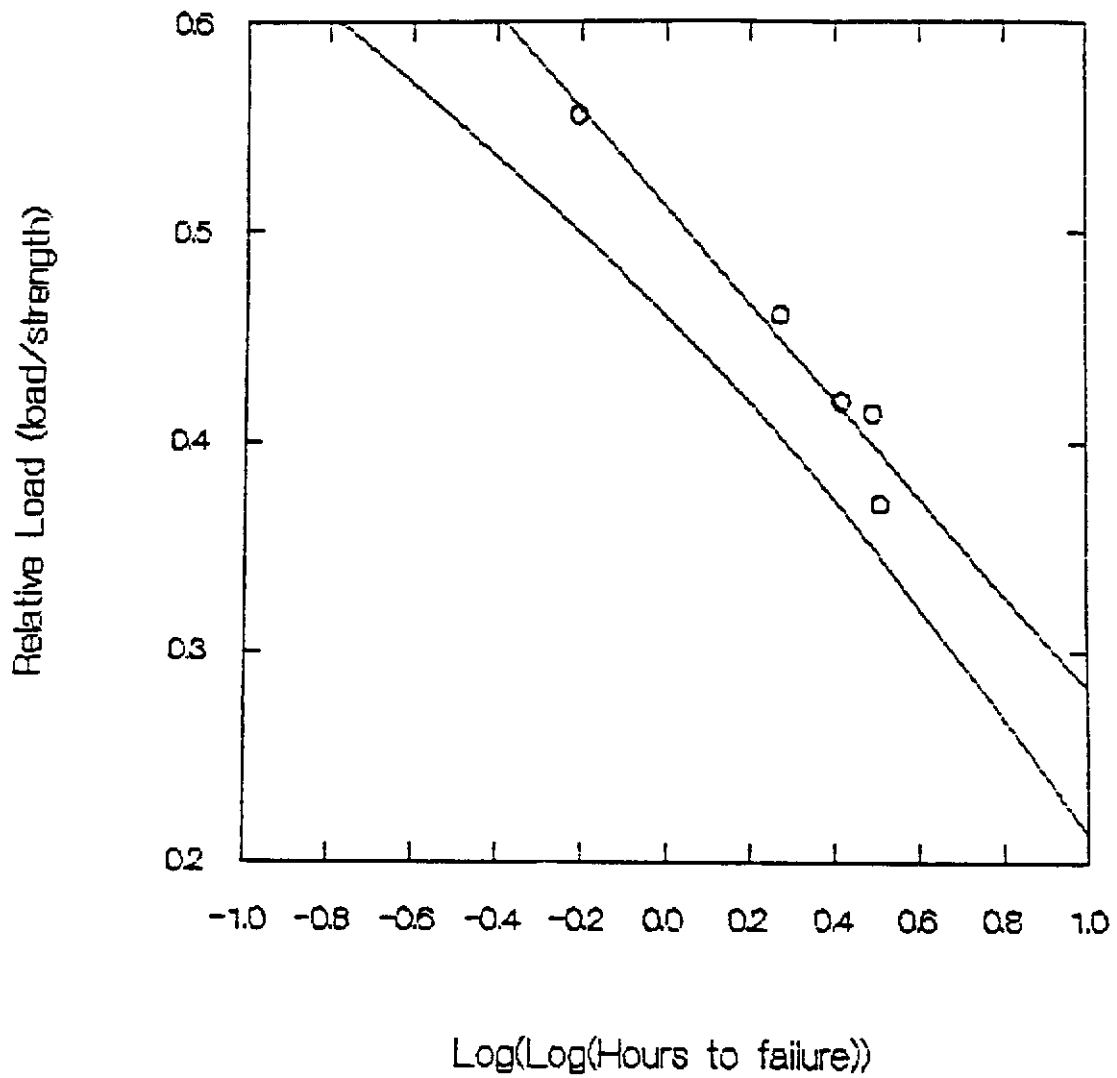


Figure 28 - Relative Load Plotted against Log (Log (Hours to Failure)) for Tensar SR2 Showing Hyperbolic Nature of Confidence Limit

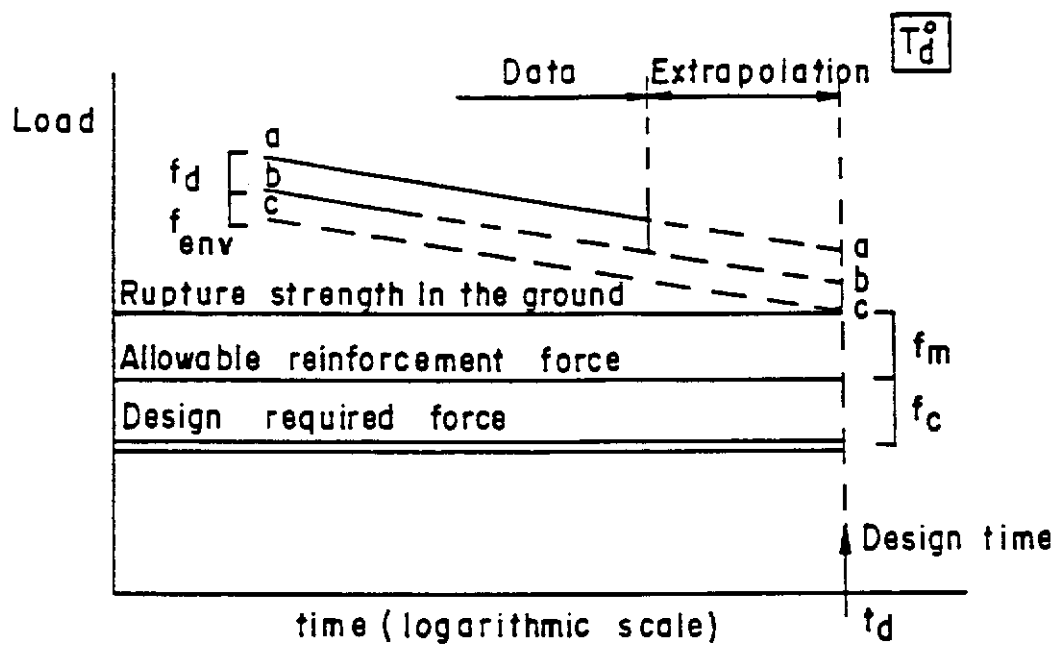


Figure 29 - Calculation of Design Required Force (See Ref. 39)